2 of 3

UNCLASSIFIED

$5 pg — $2.25

FINAL SUMMARY TECHNICAL REPORT ON THE CALENDAR YEAR 1963 RAMJET TECHNOLOGY PROGRAM

CONTRACT NO. AF 33(657)-12146

VOLUME II OF 12

AEROTHERMAL CAPABILITY OF PLASMA HEATERS HIGH PRESSURE AIR GENERATION

REPORT NO. 25,116

THE MARQUARDT CORPORATION

UNCLASSIFIED

THE Marquardt VAN NUYS, CALIFORNIA

Report 25,116

21

FINAL SUMMARY TECHNICAL REPORT ON THE CALENDAR YEAR 1963 RAMJET TECHNOLOGY PROGRAM

This Report contains a technical summary of all work accomplished from 25 January 1963 to 28 February 1964.

June 1964

VOLUME 11 OF 12

Prepared By: J. K. Totten

Checked By: J. R. Campbell

Approved By: R. E. Fisher

This Report contains the following sections:

The Marquardt Corporation VAN NUYS, CALIFORNIA

Report 25,116

FINAL SUMMARY TECHNICAL REPORT ON THE CALENDAR YEAR 1963 RAMJET TECHNOLOGY PROGRAM

June 1964

VOLUME 11 OF 12

Prepared by: J. K. Totten
Staff Engineer

Checked by: J. R. Campbell
J. R. Campbell
Program Manager

Approved by: R. E. Fisher
R. E. Fisher
Director, ASTRO

THE Marquardt CORPORATION VAN NUYS, CALIFORNIA

Report 25,116

FOREWORD

VOLUME 11 OF 12

In accordance with the reporting requirements of Contract AF 33(657)-12146, the following summary technical report is presented. The final report covers all work accomplished from 25 January 1963 through 28 February 1964.

In order to provide a report which can be more easily handled, and to meet the requirements that the materials section be "detachable" and Proposal Section V be a separable and distinct part, the final summary report has been divided into 12 volumes as follows:

VOLUME	CONTENTS	SECTION NUMBER
1	Electromagnetic Ramjet Research	IV
2	Jet Compressor Research and Ramjet Ejector Investigation	V & VI
3	Extended Mach Number SCRAMJET Investigations	VII
4	Novel Engine Installation Techniques	VIII
5	New and Novel Engine Concepts	X
6	Isotope Ramjet Studies	IX
7	Digital Computer Controls and New Control Studies	XI & XIII
8	Pure Fluid (Non-Moving Part) Control Elements	XII
9	Ramjet Structural Elements, and Non-Regeneratively Cooled Combustion Chambers and Nozzles	XVI & XVII
10	High Temperature Coated Tungsten Structures	XVIII
11	Aerothermal Capability of Plasma Heaters, and High Pressure Air Generation	XIV & XV
12	Extended Mach Number Concepts and Self-Consuming Ramjet Vehicle	XIX & XX

For ease of reading, all figures, tables, and references, have been included within the section with which they are associated. This was accomplished by prefixing all figure, table, and reference numbers with the Roman numeral of their respective section.

ACKNOWLEDGEMENTS

This report, and the studies and investigations leading to its preparation resulted from the efforts of a large team of engineers and scientists associated with The Marquardt Corporation. Since it would be impractical to list the names of all these persons, only the principal investigators are listed but with acknowledgement intended for all participants.

PROGRAM AREA	PRINCIPAL INVESTIGATORS
Aerothermal Capability of Plasma Heaters	R. C. Malneritch R. J. Page N. E. Prevatte
High Pressure Air Generation	G. R. Ranslem

VOLUME II

TABLE OF CONTENTS

VOLUME II

LIST OF ILLUSTRATIONS

VOLUME II

LIST OF ILLUSTRATIONS (Cont'd)

VOLUME II

LIST OF ILLUSTRATIONS (Cont'd)

LIST OF TABLES

OBJECT

This report is the Final Summary Technical report on the CY1963 Ramjet Technology Program and is submitted in partial fulfillment of the reporting requirements as set forth by Contract AF 33(657)-12146. This report presents a technical summary of the work accomplished during the period 25 January 1963 through 28 February 1964.

SUMMARY

The objective of the CY1963 PLASMA ARC HEATER PROGRAM was basically to design, fabricate, and test plasma heaters capable of operating at pressure levels beyond the current state-of-the-art. The experimental pressure range was to be between 1000 psia and 8000 psia. During this program all of the program goals were exceeded; one particularly outstanding test run with air at 2800 psia produced a gas enthalpy level of 3150 Btu/lb at a 0.135 lb/sec flow rate with an arc power of 1.12 Mw. This plasma arc heater has materially advanced arc heater technology. Another experimental arc heater was successfully operated at 7600 psia or approximately 200 atmospheres. This plasma heater has demonstrated the feasibility of arc heaters at extremely high pressures. This heater has also yielded information important to the design of very high pressure air breathing facility devices. An analytical study included in this year's effort has covered the feasibility of a supersonic flow arc heater. The concept of a supersonic flow heat addition arc heater is technically feasible and could possibly extend arc heater capabilities beyond presently accepted limits.

The purpose of the CY 1963 HIGH PRESSURE AIR GENERATION PROGRAM was to demonstrate the practicability of creating extremely high pressures utilizing the principle of heating a cryogenic fluid in a constant volume vessel. The numerical goal of pressure levels in excess of 50,000 psia was successfully met when one test run attained a pressure level of 62,800 psia, at a fluid temperature of 790°R. In addition, a method for obtaining and documenting pressure, volume, and temperature data at pressures in excess of currently available information was successfully demonstrated.

INTRODUCTION

The CY1963 Ramjet Technology Program was directed toward a comprehensive program of air breathing propulsion research which was aimed at providing the foundation upon which future engine development programs may be established. This program was slanted strongly toward examination of a number of promising new engine concepts while still providing a well balanced program of applied research in technological areas related to air breathing propulsion. This program was an extension and continuation of the Advanced Atmosphere-Breathing Engines and Components Program conducted under the CY1962 Air Force-Marquardt Contributing Engineering Program (Contract AF 33(600)-40809).

XIV. IMPROVEMENT OF THE AEROTHERMAL CAPABILITIES OF PLASMA HEATERS

Plasma heaters are recognized as an extremely attractive device for adding energy to a high pressure moving air stream. High air pressure and enthalpies are required in a ground test facility to simulate equivalent stagnation conditions of the airbreathing flight corridor. Research experiments have demonstrated arc heater application and have illustrated the future potential of further developing this technique of energy addition.

Previous arc heater studies have been confined to subsonic flow configurations. Studies conducted on this program have shown the feasibility of arc heater operation in the supersonic flow regime. It was shown that electric arc heater capability for simulation of hypervelocity flight conditions can be extended by operation in the supersonic flow regime. The basic reason for this extension is that the supersonic heat addition method eliminates the large radiation losses associated with the hot, low velocity chamber gas of a subsonic flow arc heater.

The CY 1963 Ramjet Technology Program on plasma heater development has analytically and experimentally evaluated three major areas: (1) supersonic arc heater analysis, (2) development and testing of a 1 megawatt, 3000 psia arc heater, and (3) design, development, and testing of a 250 kilowatt, 8000 psia arc heater.

A. Arc Heater Analysis

1. Air Heating Studies

a. Application of Vitiated Air to Experimental Studies

Vitiation (i.e. combustion) heating of gas mixtures for simulation purposes has been considered for applications toward both aerodynamic and combustion test simulation. Hydrogen and propane vitiation was summarized in curve form for final fluid temperature composition, and molecular weight, respectively, in Reference XIV-1. Vitiation was found to be a very practical simulation technique, providing the fluid composition can be accounted for in the application of the vitiated airstream to a test item.

- -

REFERENCE XIV-1 Campbell, J. R. "Second Quarterly Progress Report on the CY 1963 Ramjet Technology Program" Report Number 25,092 CONFIDENTIAL (Title - Unclassified)

b. Flight Simulation Effects for Equilibrium and Frozen Flow

The ability to simulate hypersonic flight has been evaluated for expansion of arc-chamber stagnation parameters through a convergent-divergent type nozzle. Calculations were performed with both equilibrium and frozen flow expansions of heated air to relate arc-chamber conditions to simulate flight velocities and altitudes.

Frozen flow expansion when compared to equilibrium expansion (Reference XIV-2) requires a lower total pressure (diminished molecular weight created by the pronounced freezing of atomic oxygen), and a larger total temperature (the kinetic energy must be developed from sensible energy alone, without benefit of recovered dissociated energy) for simulation purposes. Consequently, the design of a facility nozzle and selection of arc-chamber operating conditions to simulate hypersonic flight are greatly dependent upon whether the actual flow falls closer to the equilibrium or to the frozen expansion limit. Equilibrium performance of a system designed on the presumption of frozen performance will be extremely misleading. Both the velocity attained and the exit static temperature would be much greater than desired. Conversely, if frozen flow were to occur in an exhaust nozzle designed for equilibrium performance, the flow would greatly overexpand and the exit static temperature would be considerably less than expected.

2. Subsonic Flow Arc-Heater Studies

a. Effects of Magnetic Field Strength and Pressure on Arc-Heaters

Both magnetic field strength (B) and pressure (P) can strongly influence the design and operation of radial arc heaters since both factors affect the arc voltage drop. Increasing pressure raises the heat transfer to the chamber walls as is discussed in a later section. Increasing the magnetic field strength changes the arc resistance from a negative value to a positive resistance which in turn improves the arc stability. Furthermore, $(B)^2$ and (P) are fundamentally related as energy densities in the stream. The magnetic lines of force in the arc heater are at right angles to the electric potential field and in the direction of gas flow. From the analyses, the electrical discharge was shown to rotate as the flow of electrons traveled from cathode to anode. This rotation was examined with respect to B and P and reported in Reference XIV-1. The net effect of the arc rotation is a lengthened arc path that requires a greater voltage drop (and therefore lower current level) for a specific power level. This results in lower current densities, which in turn reduce electrode erosion rates.

- -

REFERENCE XIV-2 Campbell, J. R. "First Quarterly Progress Report on the CY 1963 Ramjet Technology Program", Report No. 25,087 Volume I. CONFIDENTIAL (Title - Unclassified)

3. Supersonic Flow Arc-Heater Studies

Previous studies conducted with arc heaters have been confined to subsonic configurations. This current program also considered the operation of arc heaters in the supersonic regime.

Two methods for the addition of heat to a supersonic stream were analyzed: (1) constant area heat addition; and (2) constant Mach number heat addition.

a. Constant Area Heat Addition

Constant area heat addition reduces the local Mach number and a choked condition is approached. If the added energy is too great, the steady-state flow will readjust which may involve, first, the appearance of shocks and, finally, subsonic flow. The maximum total temperature rise ratio that may be obtained and sustain supersonic flow along with the associated total pressure loss was calculated as derived in Reference XIV-3. The calculations showed that the supersonic stream must initially consist of a high total pressure and temperature to permit a practical increment of increase in enthalpy.

b. Constant Mach Number Heat Addition

Constant Mach number heat addition should be accomplished at a stream velocity slightly greater than the local speed of sound to minimize the initial total pressure requirement for flight corridor simulation of velocity and altitude. The total pressure ratio varies inversely with the total temperature ratio raised to a function of the square of Mach number, which indicates that the stagnation pressure loss is very drastic for supersonic speeds. Curves were generated as shown in Reference XIV-2, which show the supply stagnation pressure and temperature required to simulate the upper limit of the air-breathing flight corridor for Mach 1 and Mach 2 heat addition.

c. Operational Practicality of Supersonic Flow Arc Heaters

The important criteria in arc heaters designed for an electric discharge across a supersonic fluid (Reference XIV-3) are: (1) the electron drift velocity (velocity with which an electron travels from cathode to anode) between electrodes must be substantially greater than the gas velocity in the direction of flow, and (2) a sufficient

- -

REFERENCE XIV-3 Campbell, J. R. "Third Quarterly Progress Report on the CY 1963 Ramjet Technology Program". Report Number 25,109 Volume I. CONFIDENTIAL (Title - Unclassified)

density of charged particles must be maintained between the electrodes despite displacement forces. It should be noted that experimental results with $\bar{J} \times \bar{B}$ accelerators at Marquardt have already demonstrated the ability to maintain an electrical discharge in a supersonic stream.

d. Design Analysis - Supersonic Flow Arc-Heater Model

A design analysis for a supersonic flow, radial arc heater was conducted. Utilizing the constant Mach number heat addition method, supersonic flow conditions and heater geometry were determined. Arc heater analysis and parameters selected for the study were presented in Reference XIV-3. The heater nozzle design was of the convergent-divergent type with flow expanding to Mach 3. Calculations which included friction effects showed: (1) the throat area to be 0.0292 square inches, (2) the nozzle exit area to be 1.385 square inches, and (3) the area immediately upstream of the arc to be 0.0342 square inches, for an air flow rate of 0.166 lbs/sec. These areas would be much larger to accommodate flow rates required for a full scale facility arc heater. An abrupt area increase (31.7 times larger than the upstream area) will occur at the arc station to allow for constant Mach number (1.245) heat addition. A scaled version of the supersonic arc heater is presented in Figure XIV-1.

A comparison of subsonic and supersonic heat addition with flow expanding through a DeLavel-type nozzle indicated that the kinetic energy gain for both modes of operation is approximately the same. A substantial relief in heat load on the nozzle throat (cold flow) and a considerable total pressure loss was associated with the supersonic mode of energy addition. However, electric arc heater capability for simulation of hypervelocity flight conditions can be extended by operation in the supersonic flow regime. The basic reason is that there is an upper limit to energy addition that applies more strongly to subsonic operation. This upper limit is evidenced at the point where energy loss (primarily due to radiation) equals equipment ability to add energy to the air stream. Supersonic heat addition can substantially extend this upper limit, mainly because the hot subsonic mixing chamber and its associated energy loss can be eliminated.

4. A Means to Increase Total Pressure in the Supersonic Flow Arc Heater

A preliminary investigation was made with the objective of increasing total pressure by utilizing an electromagnetic accelerator connected to a supersonic flow arc heater. This would compensate somewhat for the large stagnation pressure loss associated with supersonic heat addition.

SUPERSONIC FLOW ARC HEATER

① HIGH TEMPERATURE CERAMIC
② ARC REGION-TYPICAL
③ WATER COOLED CATHODE
④ WATER COOLED ANODE
⑤ INSULATOR-TYPICAL
⑥ THROAT
⑦ CONICAL PORTION LINED WITH INSULATOR-TYPICAL
⑧ MACH 3 EXIT
⑨ FIELD COIL-TYPICAL

DESIGN WAS PREDICATED UPON ANALYSIS AND HEATER CONDITIONS GIVEN IN THE "THIRD QUARTERLY PROGRESS REPORT ON THE CY 1963 RAMJET TECHNOLOGY PROGRAM" - REPORT NO. 25,109

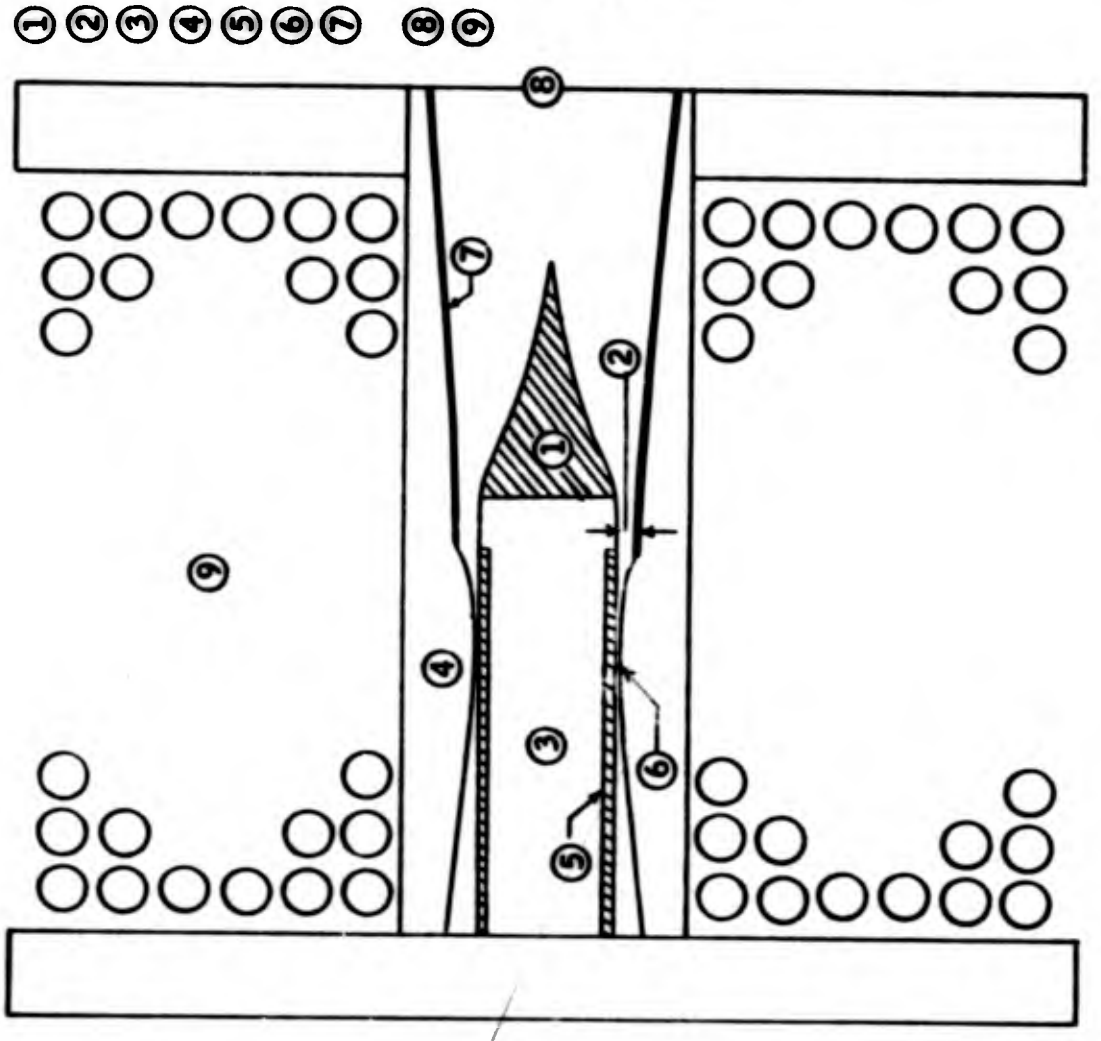

R-17,211

Figure XIV-1

In an electromagnetic accelerator, the supersonic stream of hot gas is accelerated by means of a body force (crossed magnetic and electric fields mutually perpendicular to the velocity vector) which results in a total pressure increase. This is completely in contrast to direct heating, such as arc heating or combustion where a sizeable pressure decrease occurs.

Stagnation pressure increases with increasing conversion efficiency (η). All of the electrical energy input is converted to direct kinetic energy when $\eta = 1$. Unfortunately, the channel length required to attain large pressure gains increases with increasing η and becomes infinite for $\eta = 1$ (the accelerating body force then becomes negligible).

The method of Reference XIV-4 was used with the selection of constant area channel flow. A total pressure increase of 35 percent was indicated for an initial Mach number of 3, a total temperature ratio of approximately 2.25, ratio of specific heats of 1.3, and a conversion efficiency of 60 percent. Obviously, this pressure rise is too small, however, this principle appears feasible at an initial supersonic Mach number approaching 1.

5. Radiation Losses in the Stilling Chamber of Subsonic Flow Arc Heaters

There is one distinct problem inherent in all arc heater designs, namely the survival of the arc chamber inner wall that is exposed to the hot gas. The heat flux to this inner surface is primarily caused by convection and radiation energy losses of the hot gas plus the arc foot. Convection heat transfer predominates in small subsonic arc chambers and generally reaches its maximum value in the nozzle throat. Radiation becomes more of an influence with increasing chamber volume and pressure and certainly predominates in full scale facility arc heaters. In fact, it is believed that radiation heat transfer predominates in the high pressure arc heaters of The Marquardt Corporation. Low flow velocity (less than 10 ft/sec in the arc chamber of the 3000 psi, 1 Mw electric arc heater) in the arc chamber is associated with a characteristic large radiation loss from the hot gas to the inner chamber wall.

To obtain an order of magnitude for the radiation loss of the 3000 psi, 1 Mw arc heater, a heat balance equation was written for the conservation of energy over a wide range of chamber conditions. The final form of the equation is presented on the following page:

- -

REFERENCE XIV-4 Baker, J. and Rogers, T., "One-Dimensional Magnetogasdynamic Channel Flow with Constant Conversion Efficiency", Marquardt MR 20,146, September 1961.

$$\Delta H = \frac{P_w - \epsilon V}{\dot{\omega}} \qquad (1)$$

where: P_w = Power to gas

H = Gas enthalpy addition

V = Chamber volume

$\dot{\omega}$ = Air flow rate

ϵ = Radiation intensity

The gas (air) was assumed to be in thermal equilibrium and the emissivity values of Kivel and Bailey (Reference XIV-5) were used. Reflection and re-radiation was neglected since the gas was assumed to be optically thin.

Figure XIV-2 shows gas temperature after radiation energy losses theoretically expected in the arc stilling chamber of the 3000 psi, 1 Mw arc heater as a function of power to gas, air flow rate, and chamber pressure. The radiation temperature loss is indicated for an $\dot{\omega}$ of 0.05 and 0.10 lbs/sec at a chamber pressure of 100 atmospheres. Actual experimental data of the 3000 psi, 1 Mw arc heaters are plotted on Figure XIV-2 and fall amazingly close to theory. There probably will be some difference at the higher gas temperatures partly because of rapid ionic recombination taking place (non-equilibrium) and partly because the temperature of the gas will not be uniform.

Figure XIV-3 presents the percentage temperature decrease in the arc stilling chamber due to the radiation energy loss. This plot indicates, as suspected, that radiation losses increase with decreasing velocity or with increasing pressure. The curve implies that full scale facility electric arc heaters will definitely be limited because of radiation losses unless flow velocities are great enough (supersonic flow arc heater) to have more influence than arc chamber volume.

Figure XIV-4 was constructed to indicate the influence of arc chamber volume. It is clear when comparing Figure XIV-2 to Figure XIV-4 that radiation losses greatly increase with chamber volume.

B. 1 Mw, 3000 psia Arc Heater

The experimental evaluation of the CY 1963 3000 psia, 1 Mw electric arc heater, illustrated in Figure XIV-5, has been successfully

- -

REFERENCE XIV-5 Kivel, B. and Bailey, K., "Tables of Radiation from High Temperature Air", AVCO Research Report 21, AVCO Research Laboratory, December 1957.

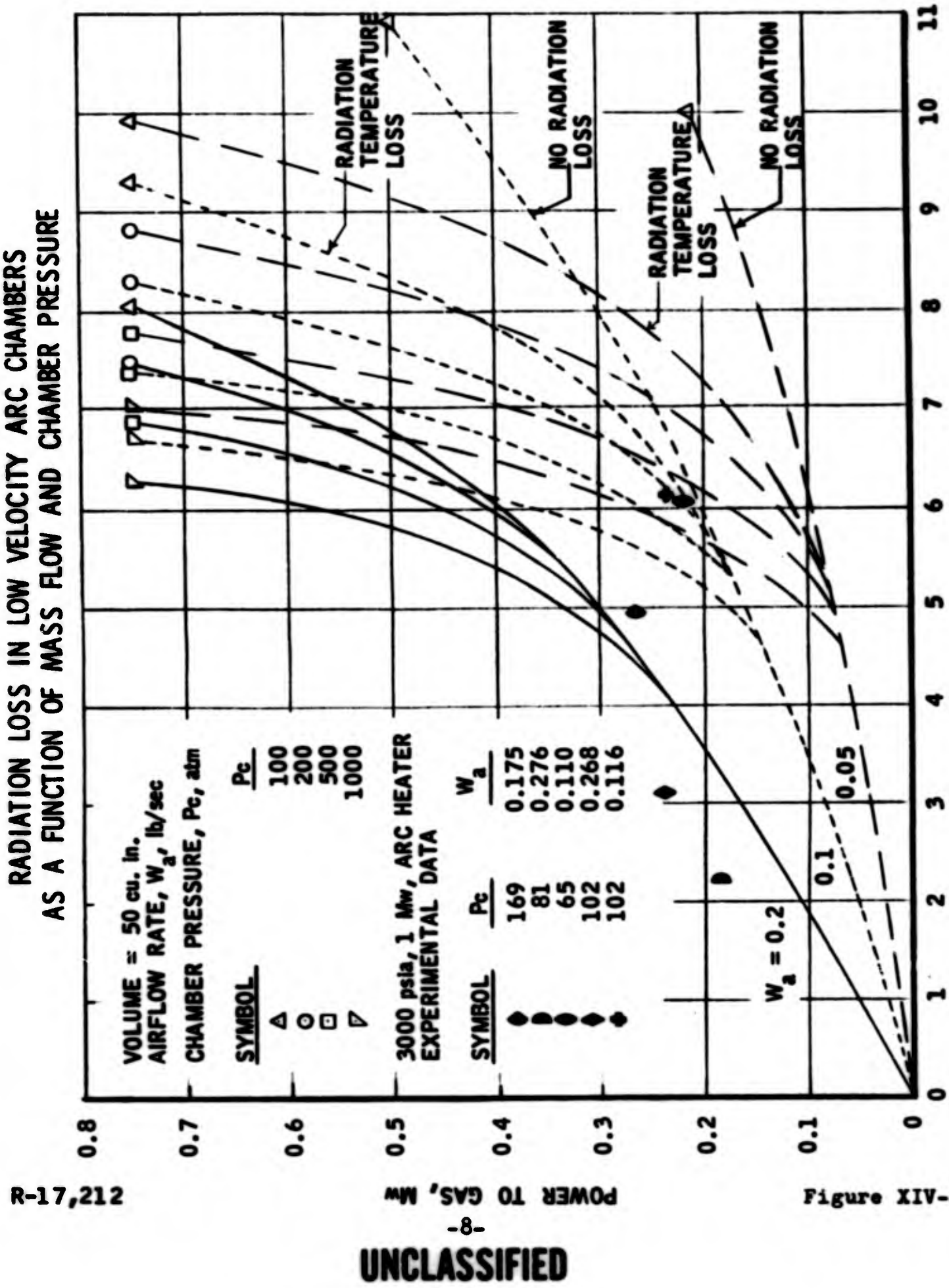

R-17,212

Figure XIV-2

THEORETICAL CHAMBER PRESSURE DECREASE RESULTING FROM RADIATION LOSSES IN A LOW CHAMBER VELOCITY ARC HEATER

VOLUME = 50 cu. in.

AIRFLOW RATE, lb/sec	SYMBOL	CHAMBER PRESSURE, atm
——— 0.2	△	100
- - - - - - - - 0.1	⊙	200
—— —— —— 0.05	□	500
	▽	1000

$T_{rad.}$ = TEMPERATURE AFTER RADIATION LOSS

T_{ideal} = TEMPERATURE WITH ZERO RADIATION LOSS

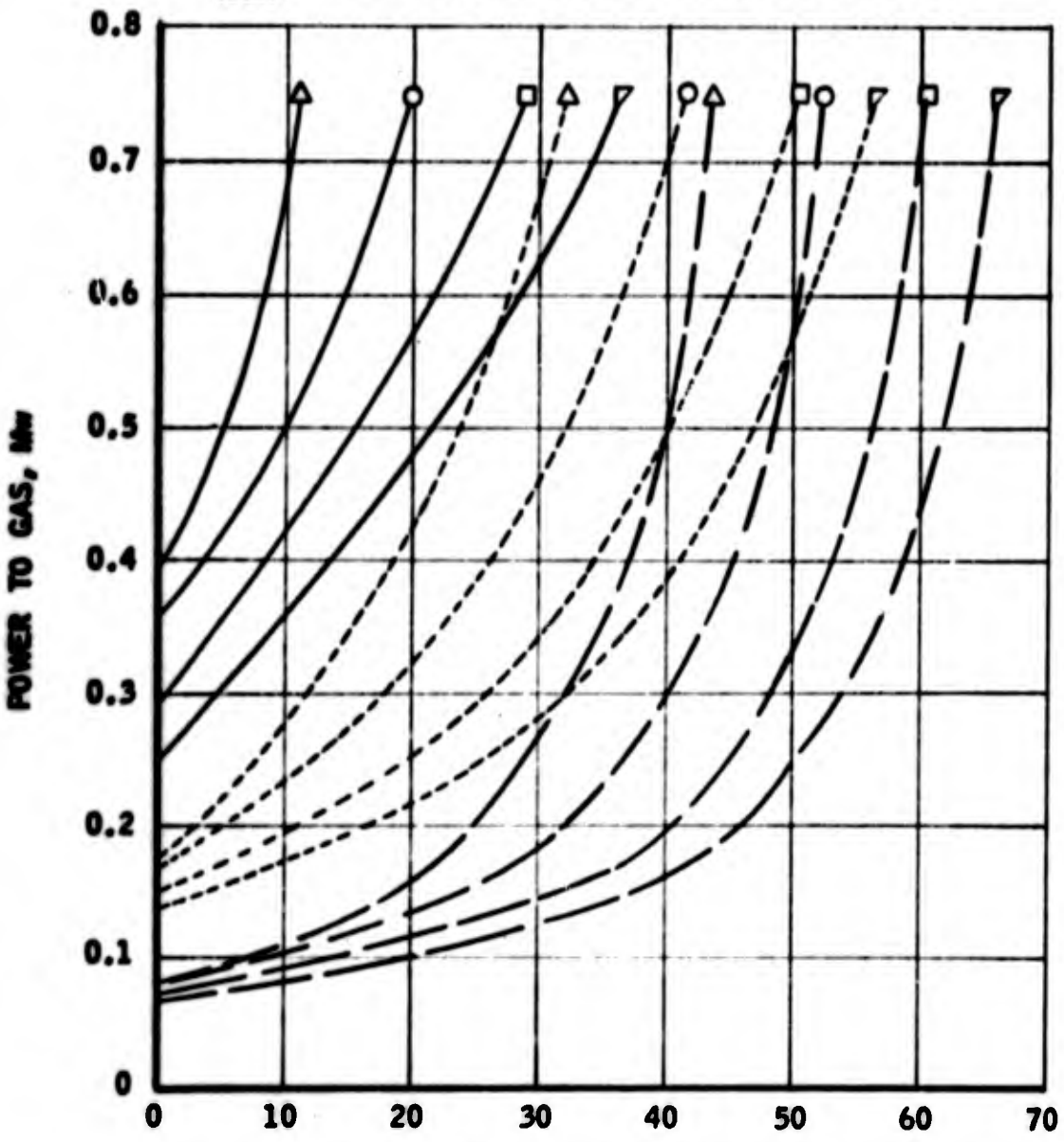

R-17,213

Figure XIV-3

BLANK PAGE

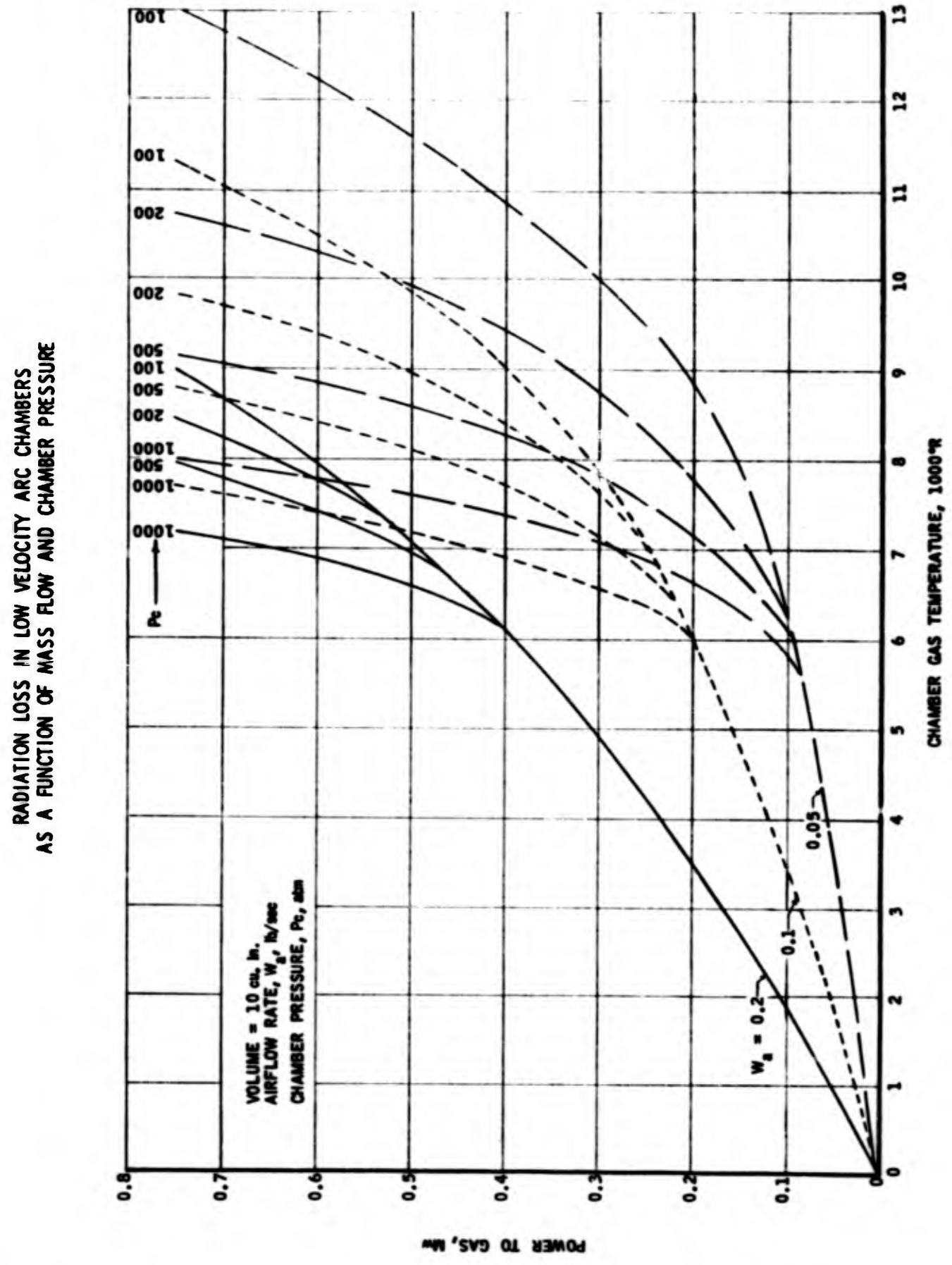

R-17,214

FIGURE XIV-4

3000 PSIA, 1 Mw ARC HEATER

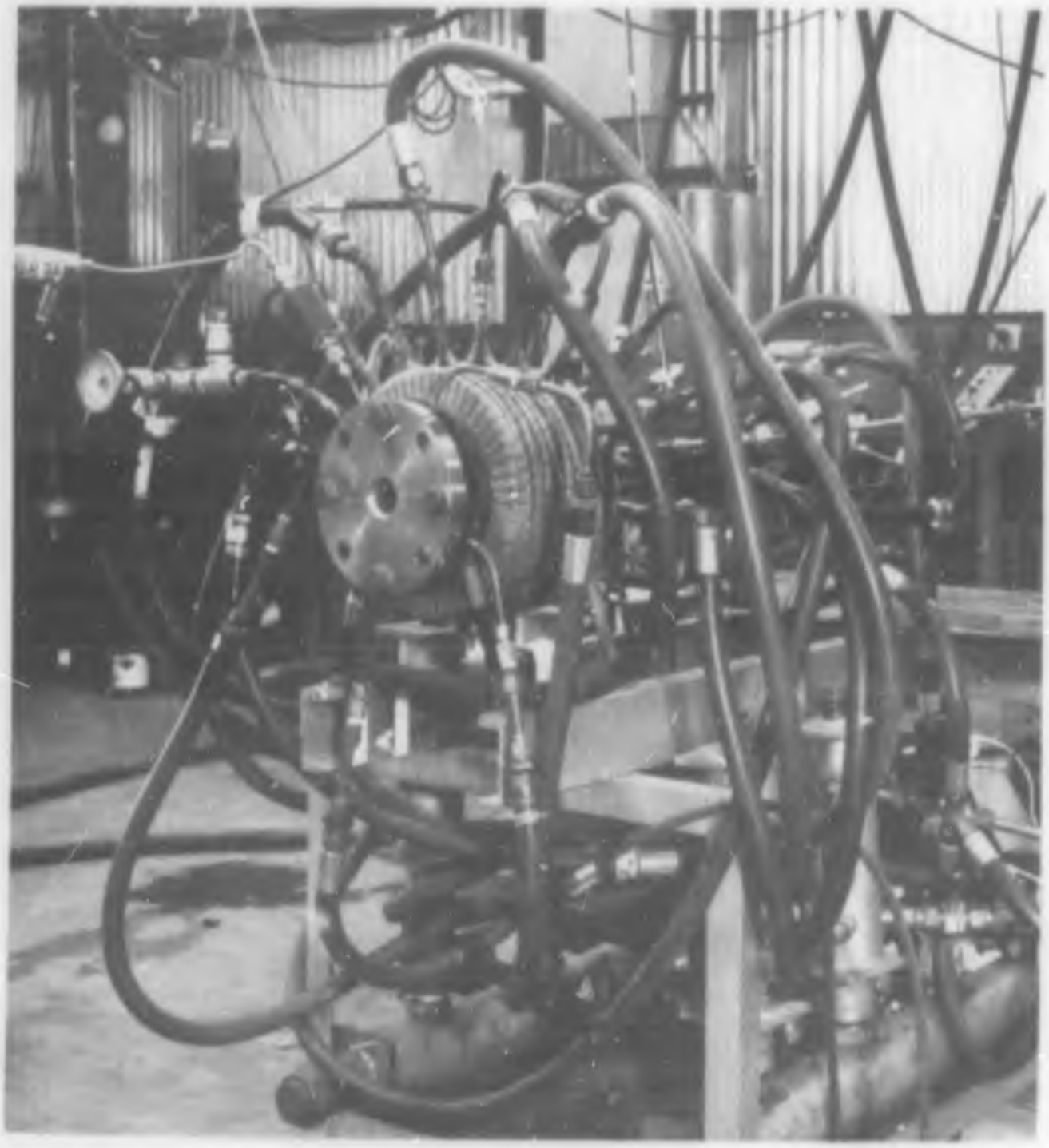

R-17,202
Neg. T5123-1

FIGURE XIV-5

completed. The experimental program consisted of 15 test runs completed at The Marquardt Field Research Laboratory, Saugus, California. The heater was operated with air at pressures in excess of 2800 psia, at a power level of 1.12 Mw and an enthalpy addition of 3150 Btu/lb to the gas. Figure XIV-6 is an assembly drawing of the tested unit. The data taken from the experiments conducted with this unit are tabulated in Table XIV-I and are described herein in paragraph B.4.

Figure XIV-7 displays the location of several of the significant data points with respect to a typical airbreathing flight corridor. The shaded section indicates the area of the flight corridor over which arc heater operation has been demonstrated.

1. Electrode Design and Performance

The outer electrode, or anode was made of four spirally wound water cooled copper tubes as shown in Figure XIV-8. On several occasions, the arc traveled upstream and burned off the tubing at the inlet flange. This appears to have been caused by the attachment of the power lead at the downstream end of the heater. An analysis of the forces developed by current carrying conductors shows that the arc will tend to be forced to the end of two parallel conductors when the power leads are attached at the same end. A subsequent re-connection of the anode power lead to the inlet end of the heater eliminated this problem and on later runs the arc attached and held to the downstream end of the cathode as desired.

The center electrodes utilized are of the same design previously used. The heavy walled copper tubing was replaced with a monel tube to permit operation at the higher pressure levels. In addition, some changes were made in the facility water system which allowed increasing the cooling water pressure to over 500 psi. This increased the anode and cathode flow rates as well as providing some assistance in the structural integrity.

2. Heater Pressure Case

The outer pressure case is constructed of type 321 stainless steel. This material was selected to provide adequate structural strength in addition to being non-magnetic. It is essential to have the case constructed of a non-magnetic material to avoid undesirable distortion of the magnetic field in the arc chamber area.

3. Magnetic Field Coil

The original magnetic field coil of water cooled copper tubes wound in layers was replaced by a pancake type winding

A

UNCLASSIFIED

PLASMA ARC HEATE

3000 PSIA — 1.0 MW

HEATER 2

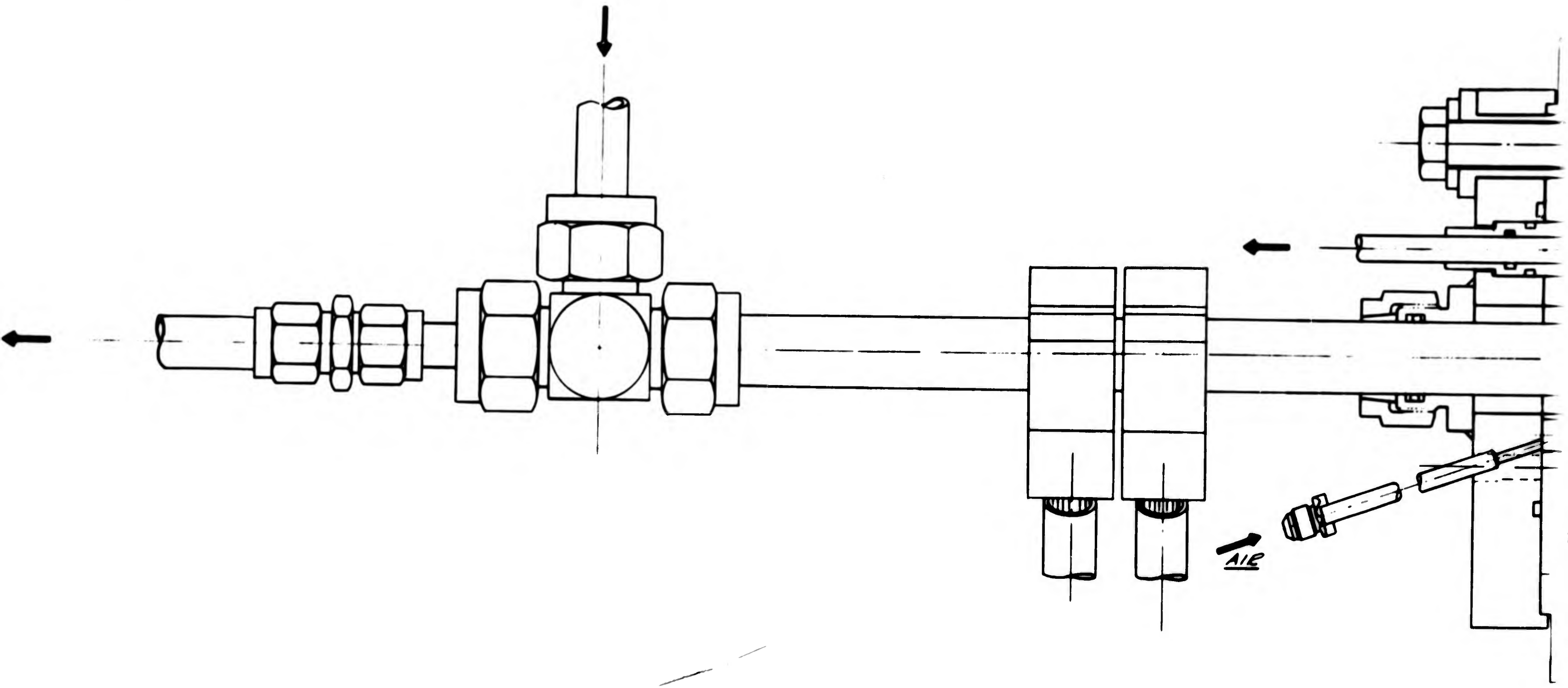

R-16,743

PLASMA ARC HEATER

3000 PSIA — 1.0 MW

REPORT 25,116

HEATER 2

B

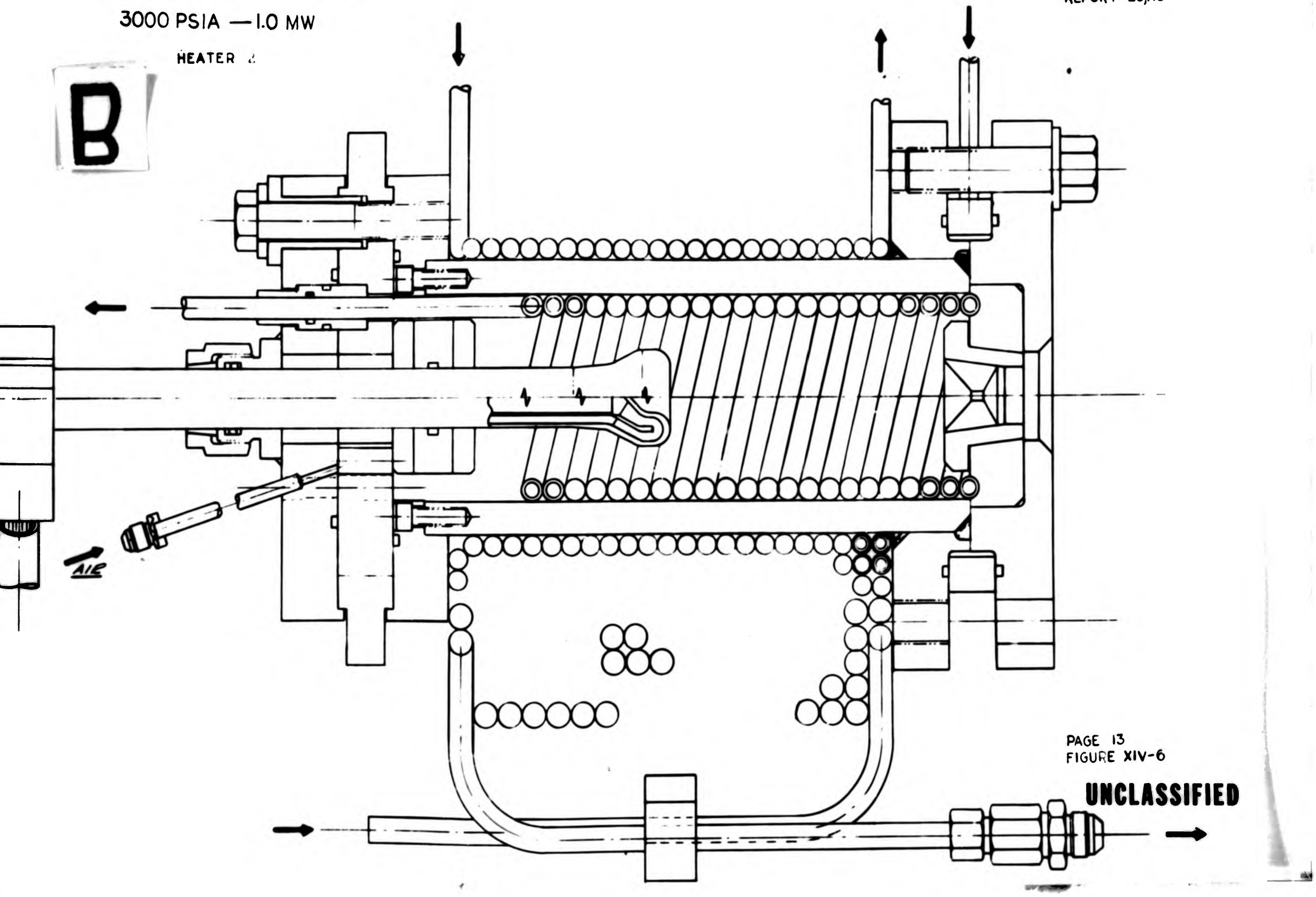

PAGE 13
FIGURE XIV-6

UNCLASSIFIED

TABLE XIV-I

200 ATMOSPHERES - 1 Mw ARC HEATER PERFORMANCE

Run	Gas	Chamber Pressure, Psia	Power, Kw	Gap In.	Gas Flow lb/Sec	Field Strength Gauss	Enthalpy Addition Btu/lb	Arc Eff. %	Overall Eff. %	Run Time Sec	
1	Air	650	605	0.5	0.058	17560	-	-	-	2.5	(1)
2	Air	500	-	0.5	-	19000	-	-	-	0.5	(1)
3	Air	500	500	0.5	-	19000	-	-	-	1.5	(2)
4	Air	735	445	0.5	-	19000	-	-	-	10	(3)
5	Air	1495	650	0.5	0.268	19000	840	37	30	20	
6	Air	1195	575	0.5	0.276	19500	630	32	25.5	20	
7	N_2	1200	510	0.5	0.225	15100				3.6	(3)
8	N_2	1540	606	0.5	0.282	15100				5.3	(3)
9	N_2	950	700	0.5	0.11	18000	1880	31.5	26.8	16	
10	N_2	1250	640	0.5	0.10	9000				5	(1)
11	Air	750	500	0.5	0.08	15400				1.5	(3)
12	Air	2480	760	0.5	0.175	15400	1440	35	31	10	
13	Air	1500	700	0.5	0.116	15200	1910	33.5	29.6	6	
14*	Air	2900	968	0.5	0.106	15700	3020	35.4	31	3	(4)
15*	Air	2800	1120	0.5	0.135	16400	3150	40	36.5	6	(4)

(1) Anode burned out terminating test
(2) Anode water line broke
(3) Arc blew out
(4) Cathode clamp failed

*with pressure sealing modifications

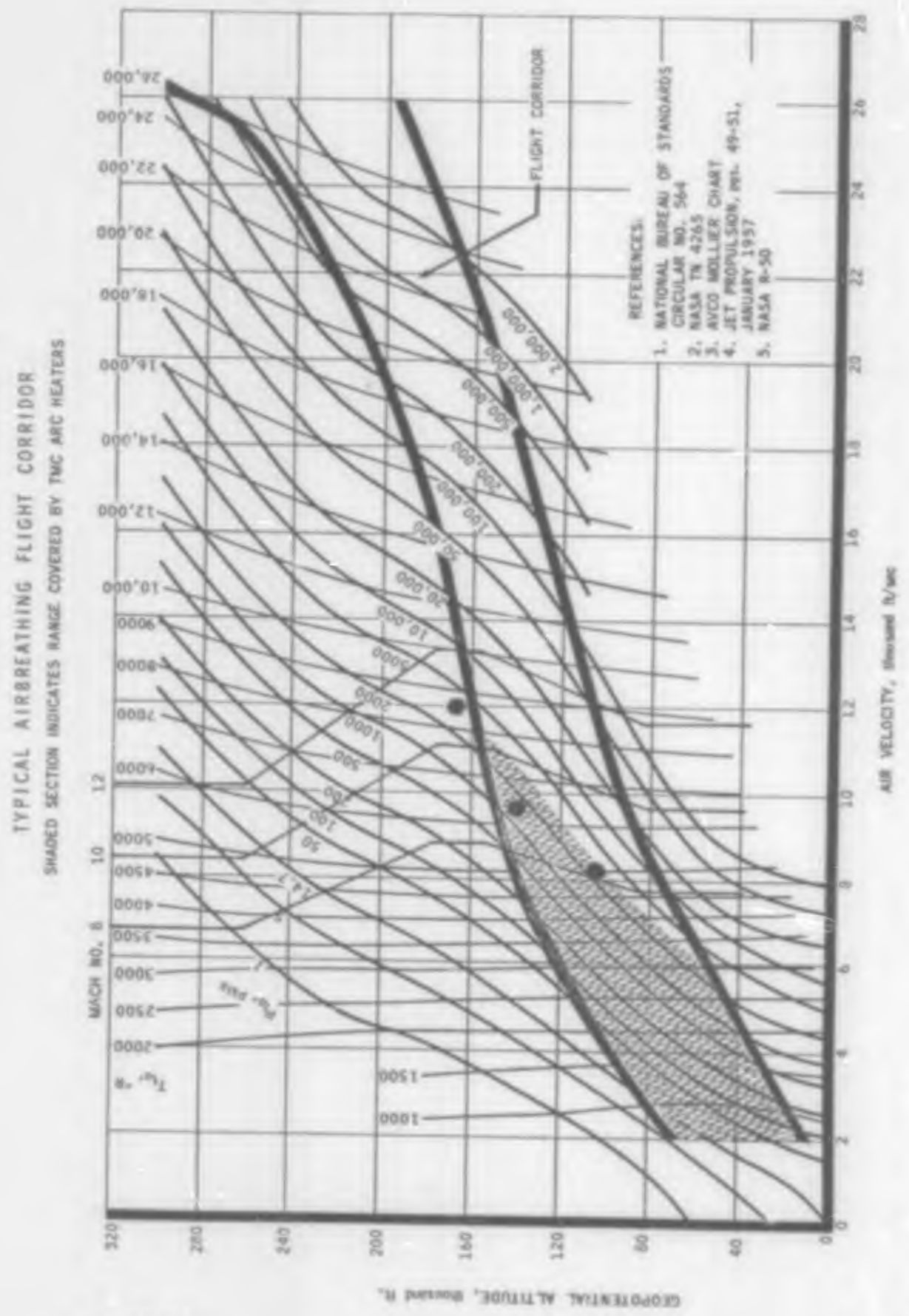

R-17,210

Figure XIV-7

ARC HEATER OUTER ELECTRODE
AFTER TEST

164.6 sec RUN TIME **REUSABLE**

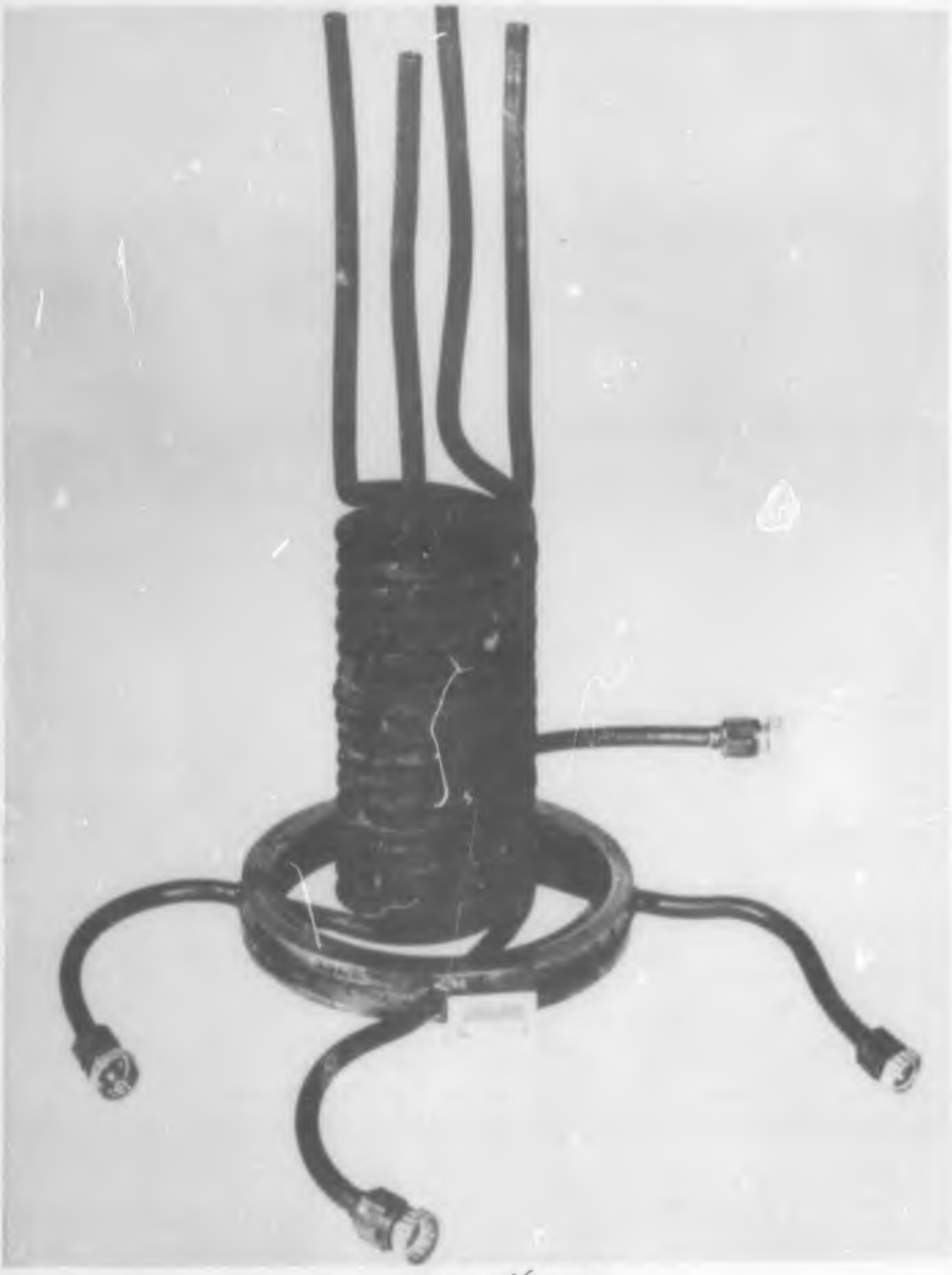

R-15,230

FIGURE XIV-9

which was assembled of several sections, each being two rows thick. A single section of the coil is shown in Figure XIV-9. The tubing used was a square tube with a round hole. This tubing has a much greater copper area, resulting in a lower power loss in the coil for a given field strength. A picture of the assembled heater with this coil installed was shown in Figure XIV-5. The magnetic field strength of this coil was checked and is shown in Figure XIV-10. The tests were conducted with a field strength ranging from 9,000 to 20,000 gauss. A plot of the actual field pattern around the arc head was made with iron filings and is shown in Figure XIV-11.

4. Experiments

A total of 15 successful experimental tests were conducted with the 3000 psi, 1 Mw arc heater at The Marquardt Research Field Laboratory, Saugus, California. The data tabulated in Table XIV-I summarizes the significant conditions met on each of the test runs.

Tests 1 through 13 consisted of a series of runs during which an attempt was made to successively increase the pressure and power until the target of 1.0 Mw, and 3000 psi operation was realized. During this group of runs a maximum pressure of almost 2500 psia was attained, however, at this pressure level the rear pressure seals failed. Many problems occurred during this series of tests, mainly with the insulator and pressure seals at the upstream end. Following run No. 13 the inlet end of the heater was modified to provide a more positive pressure seal. This was accomplished by completely eliminating the large diameter flat insulator between the pressure case and the flange that supported the center electrode.

The center electrode was then provided with an insulator around it in the area of its supporting flange. Various types of seals were tried between the flat metal flanges with little success at the high pressure levels (over 2000 psi). Finally, an "O" ring was fabricated from copper tubing and this held the chamber pressure to 3000 psi with very little leakage.

The selection of an insulator for the cathode also presented a considerable problem. It was necessary to obtain a structurally sound, high temperature electrical insulator. A 1/8 inch wall mullite tube was selected and epoxied to the cathode. It was found that the "O" ring in the Lenz fitting would not provide an adequate seal at the higher pressure levels against this ceramic surface. The gap was then filled with an epoxy which solved this leakage problem.

Run 14 was ignited at the maximum available pressure (2900 psi) and operated for 3 seconds at which time the clamp holding

HIGH PRESSURE ARC HEATER
FIELD COIL PANCAKE LAYER

R-17,203
Neg. 4832-1

FIGURE XIV-9

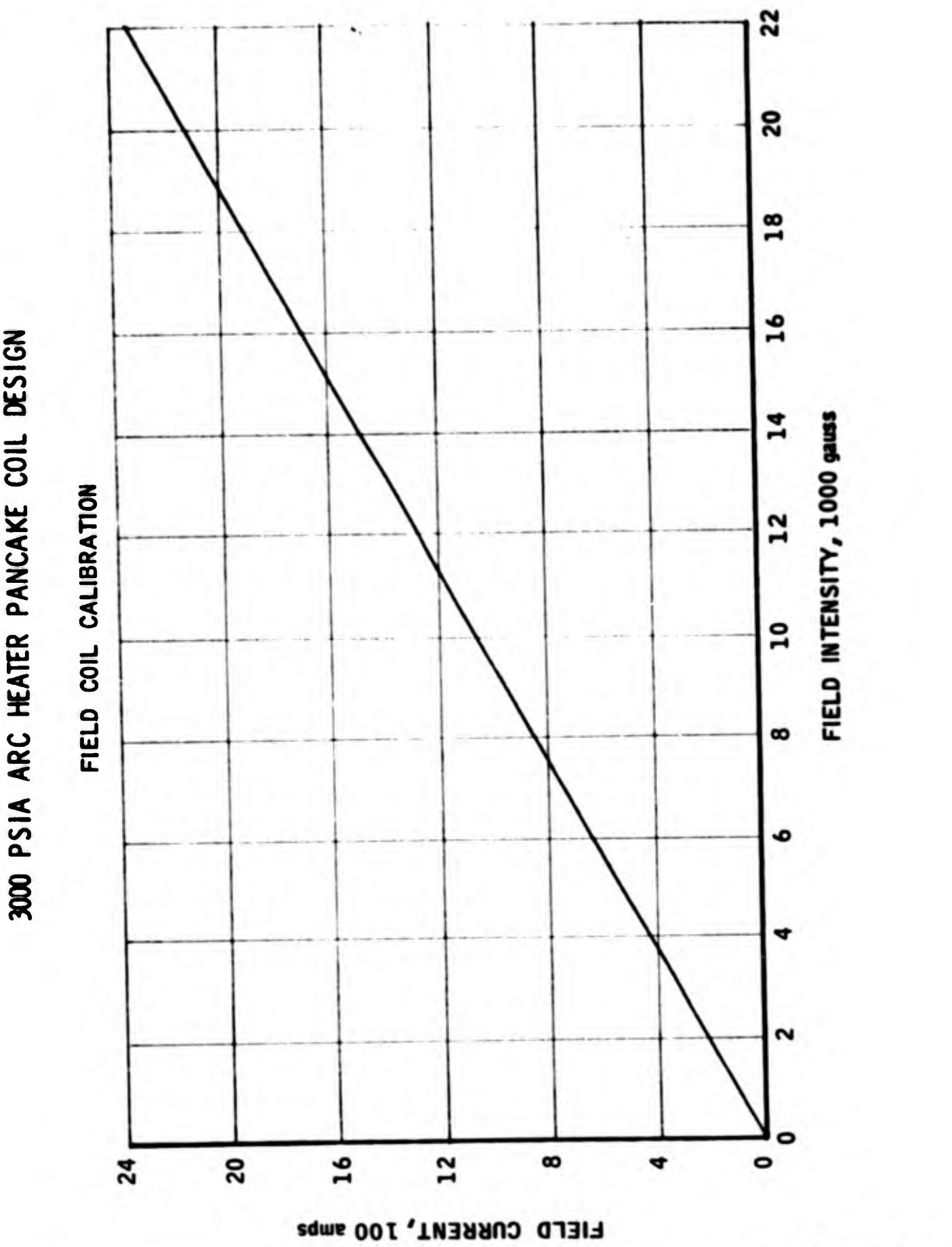

R-17,215

Figure XIV-10

3000 PSIA, 1 Mw ARC HEATER
MAGNETIC FIELD PATTERN

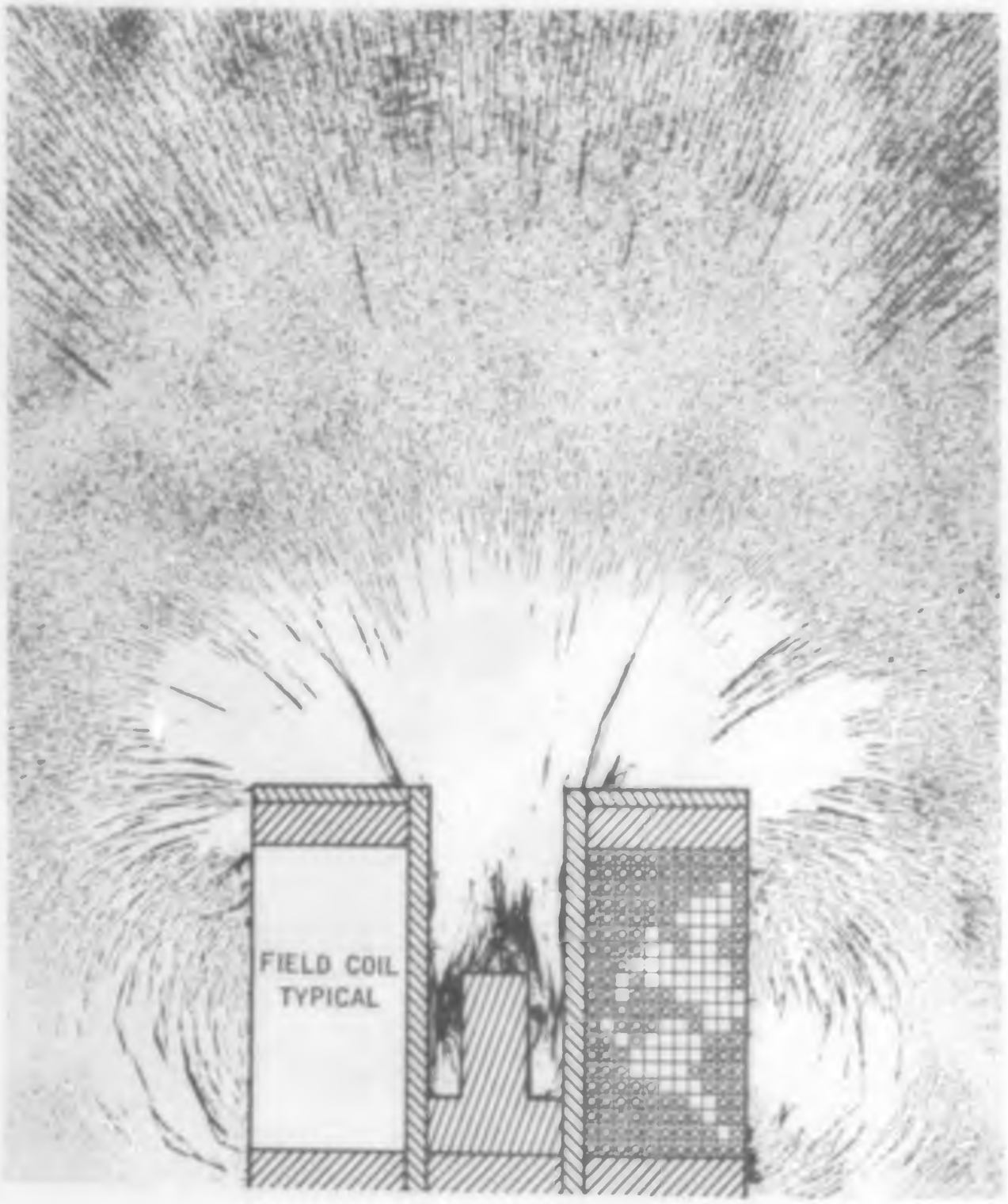

R-16,002A
Neg. CA4927-6

FIGURE XIV-11

UNCLASSIFIED

the cathode slipped, permitting the cathode to slide out the back and release the pressure. The run was terminated with only minor damage to the cathode. A power level of 968 Kw was reached on this run with an estimated enthalpy addition to the gas of 3020 Btu/lb attained. The estimated performance was based on maximum temperature rise data extrapolated from the first 3 seconds of run time.

The heater was reassembled and prepared for another test at the target conditions. Run 15 was made with ignition occurring at approximately 2700 psi. The pressure rose to 3040 psi, during start-up, and settled back to 2800 psi for the remainder of the run as this was the maximum available pressure from the facility supply. The power level on this run was 1.12 Mw, resulting in an enthalpy addition to the air of 3150 Btu/lb.

The enthalpy addition to the gas was calculated from heat balance considerations. The electrical power to the heater was measured by facility power instrumentation, consisting of shunts and transductors for current, and transductors for voltage. Both parameters were recorded on an oscillograph. The cooling water flow rates were measured with turbine-type flow meters. Flow values were read on visual meters, and recorded just prior to the test run. The temperature rise of the cooling water was measured with differential temperature transducers, and recorded on strip chart recorders. Air flow rates were calculated from pressure measurements across a flow venturi previously calibrated in the range of interest. A tracing of the oscillograph record from run No. 15 is included as Figure XIV-12. The temperature rise data for the anode and cathode are replotted in Figure XIV-13.

Run 15 lasted 6 seconds; the arc current, voltage, and the chamber pressure reached steady state conditions at approximately 2 seconds after ignition. These steady state conditions were maintained for the next 4 seconds of the run. The anode and cathode cooling water temperatures had reached 95 percent of their final value after approximately 3.25 seconds, leaving about 2.75 seconds of steady state (less than 5 percent change) run time prior to termination of the test. The test was terminated at 6 seconds because of a mechanical failure of the epoxy cementing the cathode to the insulator. The stable operation of the unit under these test conditions (see Figure XIV-12) clearly meets the goal of operating an arc heater with air at 200 atmospheres, a power level of 1 Mw, with an enthalpy addition to the gas of over 3000 Btu/lb. It is confidently expected that an improved method of securing the cathode in the heater will permit much longer run times. It is also apparent that certain minor modifications in the arc heater design, (based on experience with the 8000 psi arc heater) utilizing improved pressure seals and insulator installation and possibly different insulator materials would be required, prior to continued testing or use of this specific heater.

C. <u>High Pressure Arc Heater, ½ Mw, 8000 psia</u>

The experimental study of the high pressure (8000 psi, 250 Kw) arc heater has been successfully completed. The arc heater

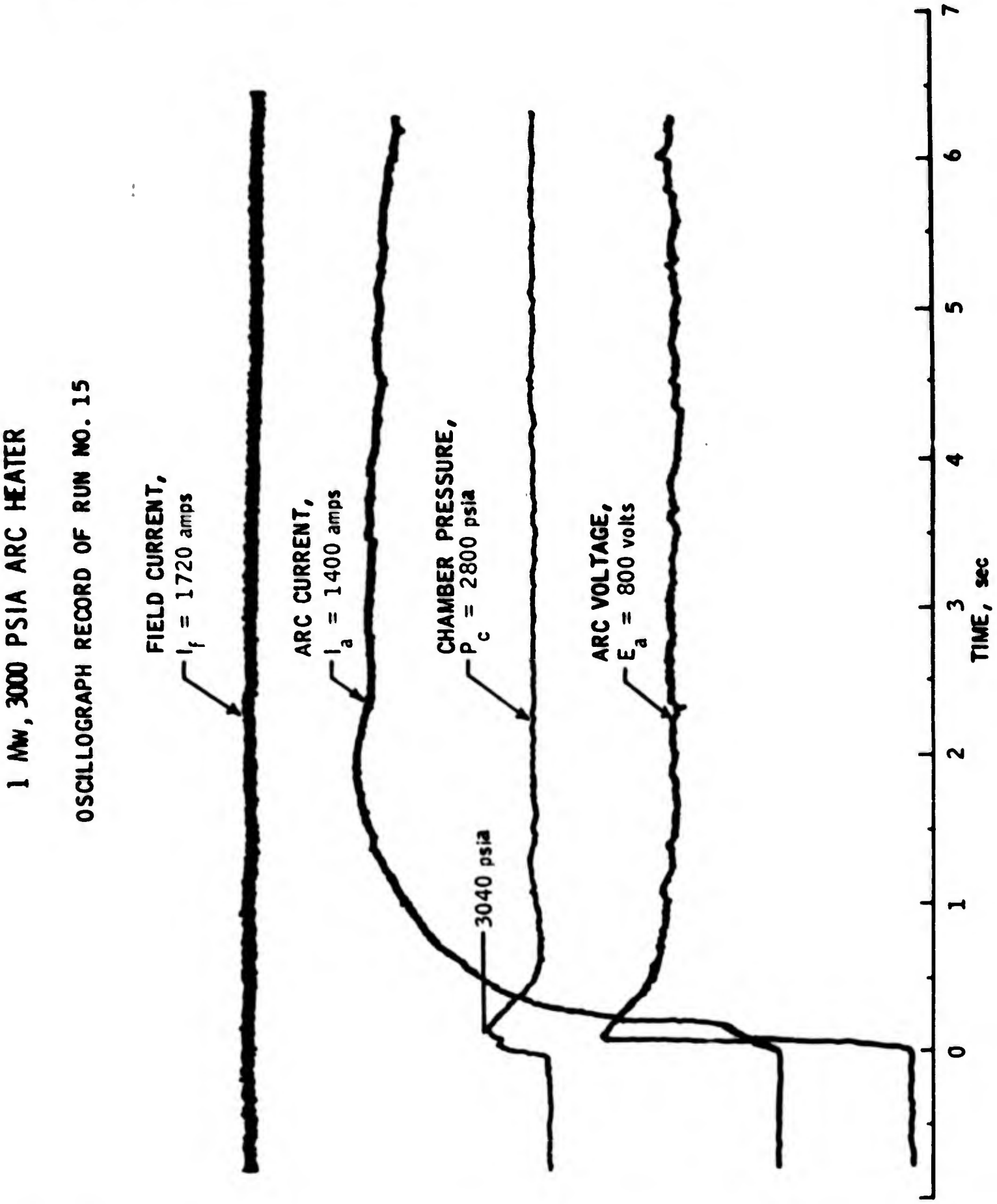

R-17,222

Figure XIV-12

1 Mw, 3000 PSIA ARC HEATER

STRIP CHART RECORD OF COOLING WATER TEMPERATURE RISE

ANODE WATER FLOW = 7.6 lb/sec

CATHODE WATER FLOW = 7.4 lb/sec

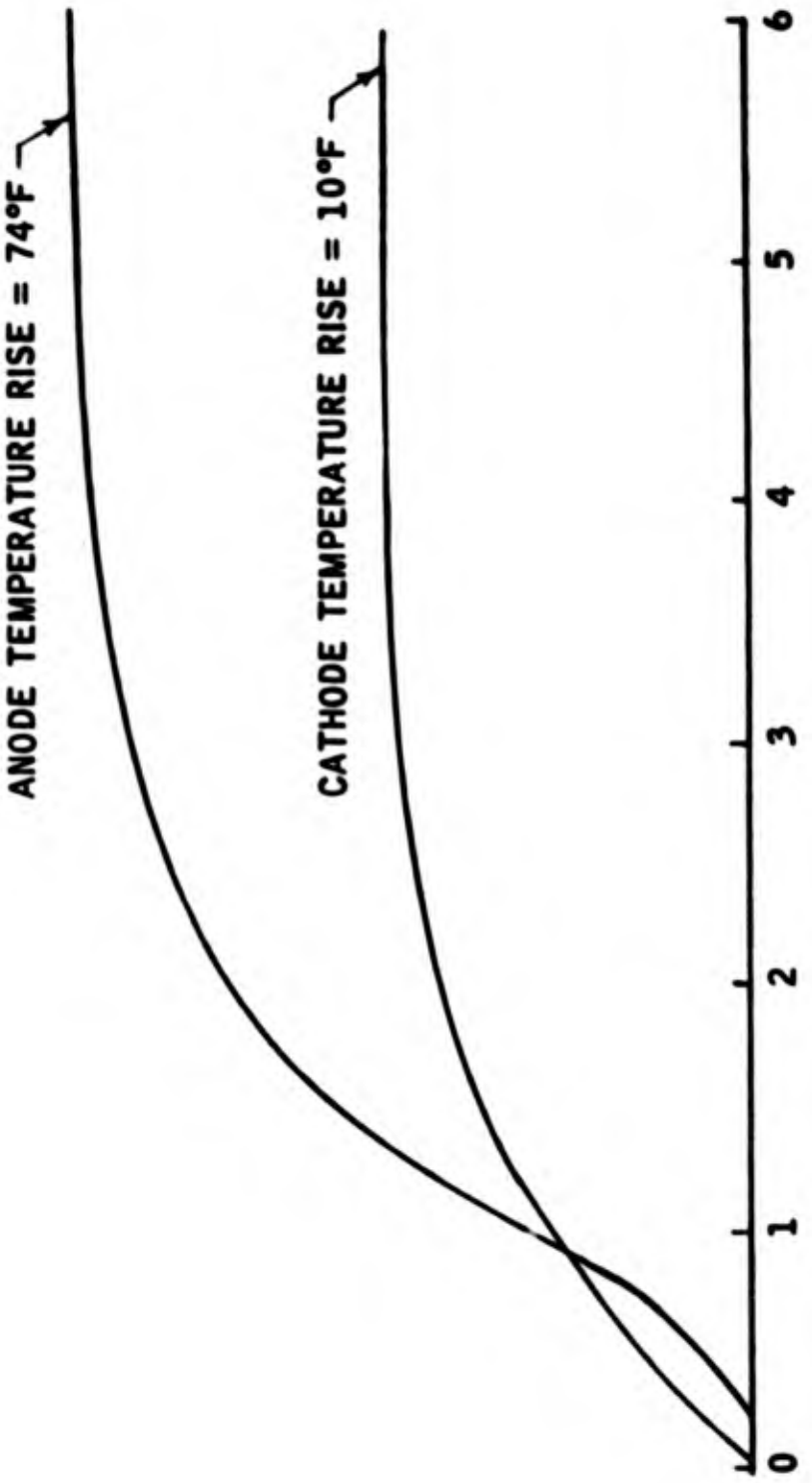

design, fabrication, and experimental program was accomplished during the latter half of CY 1963. The program followed the completion of the CY 1962 arc heater program which was extended to August, 1963.

The tests conducted under the 1962 exploratory high pressure arc heater program extension indicated the need for water cooling of both the center (cathode) and outer (anode) electrodes. The arc heater utilized during the 1963 program incorporated water-cooled electrodes.

A total of seven runs were made during the test of the high pressure arc heater. The test results definitely satisfy the primary objective of the test program, "obtaining arc operation at extremely high chamber pressures". Maximum, steady chamber pressures of 7600 psig with nitrogen as the test gas, and 7400 psig with air, were achieved with arc operating times of 20 and 14 seconds, respectively. These tests demonstrated the durability of the high pressure arc heater hardware, although a failure of the anode occurred during the last run. The damage to the anode occurred during a test to investigate the effect of increased arc current on arc voltage requirements.

An arc heater efficiency of approximately 9 percent was noted during the test run with air, with a corresponding gas temperature of 2100°R. Although the numbers presented above are relatively low, by previous arc heater standards, the ease in obtaining arc operation at the high pressures indicates higher values of efficiency and more power to the gas can be expected by increasing the arc gap and by optimizing the chamber design. Higher gas enthalpies could also be achieved by reducing the mass flow. An assembly drawing of the 8000 psia arc heater with the heat exchanger attached is shown in Figure XIV-14. Figure XIV-15 is a more detailed view of the arc heater showing the location of the outer electrode. A photograph of the assembled arc heater with the outer electrode assembly partially removed is shown in Figure XIV-16.

1. Electrode Design and Performance

The outer electrode (anode) consisted of five spirally wound water-cooled copper tubes, shown assembled to the arc heater forward flange in Figure XIV-17. The performance of the outer electrode assembly was excellent for the first six test runs. Failure of the anode occurred during Run No. 7 when the arc current was increased to investigate arc voltage characteristics. The anode melted in half and welded to the outer case. A slight erosion of the outer case also occurred. The previous six runs, during which 75 seconds of arc operation was obtained with the anode, undoubtedly contributed to the failure through the slight, continual erosion of the anode inherent during high pressure arc operation. An easily accomplished repair to the arc heater, consisting of brazing a new anode to the forward flange, would permit further testing.

BLANK PAGE

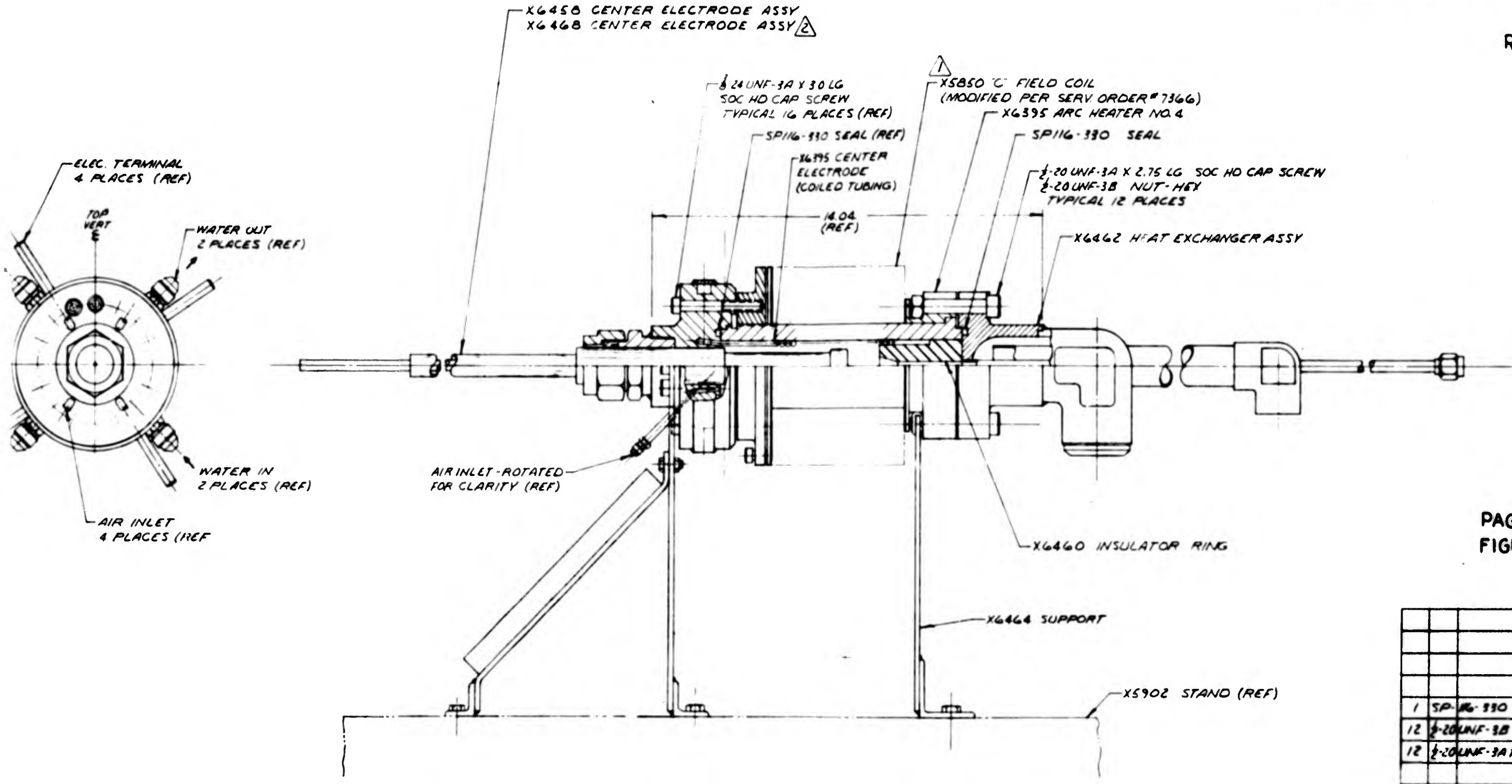

PAGE 25
FIGURE XIV-14

					20
					19
					18
					17
1	SP-116-330		SEAL		16
12	⅜-20UNF-3B		NUT - HEX		15
12	⅜-20UNF-3A X 2.75		SOC HD CAP SCREW		14
					13
1	X6469		SUPPORT		12
1	X6464		SUPPORT		11
(2) 1	X6468		CENTER ELECTRODE ASSY		10
1	X6458		CENTER ELECTRODE ASSY		9
1	X6462		HEAT EXCHANGER ASSY		8
1	X6460		INSULATOR RING		7
1	X6395		ARC HEATER NO. 4		6
1	X6850		"C" FIELD COIL		5
					4
					3
					2
					1

X6463

ASSY & INSTALLATION
ARC HEATER NO. 4
Astro
X 6463 A

(2) THIS ELECTRODE TO BE USED AS AN ALTERNATE
(1) WRAP ARC HEATER, AREA OF COIL, WITH ASBESTOS INSULATION
NOTES: UNLESS OTHERWISE SPECIFIED

PLASMA ARC HEATER
8000 PSIA — 0.15 MW
HEATER 4

REPORT 25,116

UNCLASSIFIED

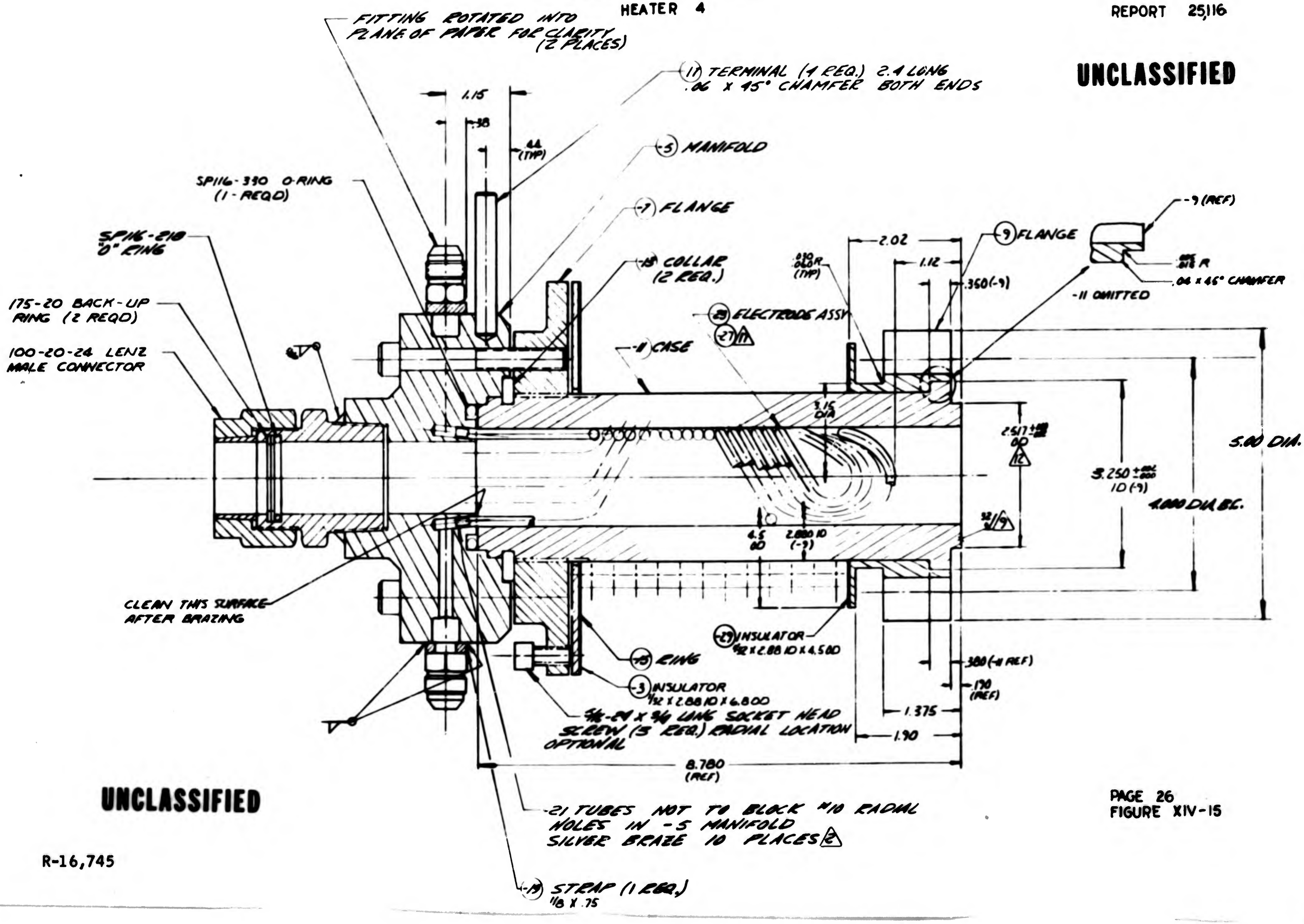

UNCLASSIFIED

R-16,745

HIGH PRESSURE (8000 PSIA) ARC HEATER
EXPLODED VIEW

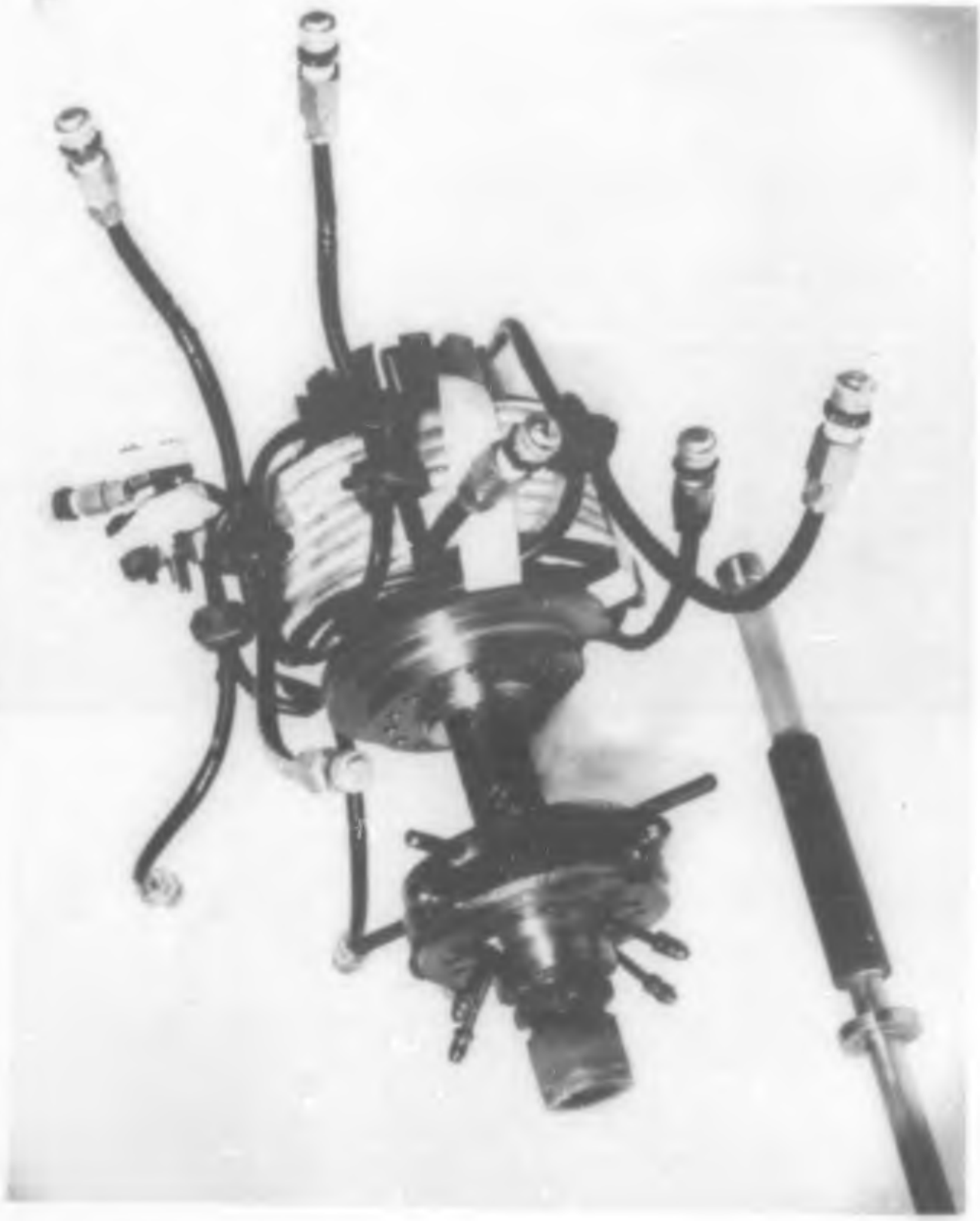

R-17,204
Neg. 4927-7

FIGURE XIV-16

HIGH PRESSURE (8000 PSIA) ARC HEATER
OUTER ELECTRODE (ANODE) AND MANIFOLD ASSEMBLY

R-17,205
Neg. 4927-9

FIGURE XIV-17

The water-cooled, thick-walled copper center electrode (cathode), used during the first six runs, is shown in Figure XIV-18. (Also shown is the tubular copper cathode used during Run No. 7). Performance of the thick-walled copper cathode was satisfactory. The top cathode of Figure XIV-19 shows the condition of the cathode used during Runs 1 and 2 following 16 seconds of arc operation. The erosion shown is attributed to inadequate cooling at the downstream edge which allowed the arc to erode the cathode to an equilibrium shape. An identical center electrode was installed and used for Runs 3 through 6. Visual observation of the cathode following Run No. 3 indicated the erosion was similar to that noted following Run No. 2. Following each run, subsequent to Run No. 3, a slight continual erosion of the cathode was noted. The bottom cathode of Figure XIV-19 shows the condition of the cathode used during Runs 3 through 6 and shows the copper oxide deposits and the total erosion following approximately 54 seconds of operation. Visual observations indicate that the majority of the erosion of this cathode occurred during the test run with air (Run No. 6). Figure XIV-20 presents a sectioned view of the cathodes shown in Figure XIV-19.

Sufficient operating time was not obtained with the tubular ring cathode to permit an evaluation of its structural performance.

2. Heater Pressure Case

The outer case was constructed of 19-9DL stainless steel. This material was selected for its structural strength and non-magnetic property. The case must be non-magnetic so that it does not influence the magnetic flux lines produced by the field coil required to induce arc rotation.

3. Magnetic Field Coil

The magnetic field coil consists of seven rows in depth of water-cooled copper tubing. This field coil is the same one used during the CY 1962 arc heater program except that the center coil was removed for installation on the new heater pressure case. Figure XIV-21 shows the field strength calibration measurements.

4. Support Equipment

The support equipment utilized for the test program consisted of:

a. A high pressure air supply system including a 12,000 psia compressor and gas storage system (0.5 ft^3), with a pressure regulator at the discharge.

BLANK PAGE

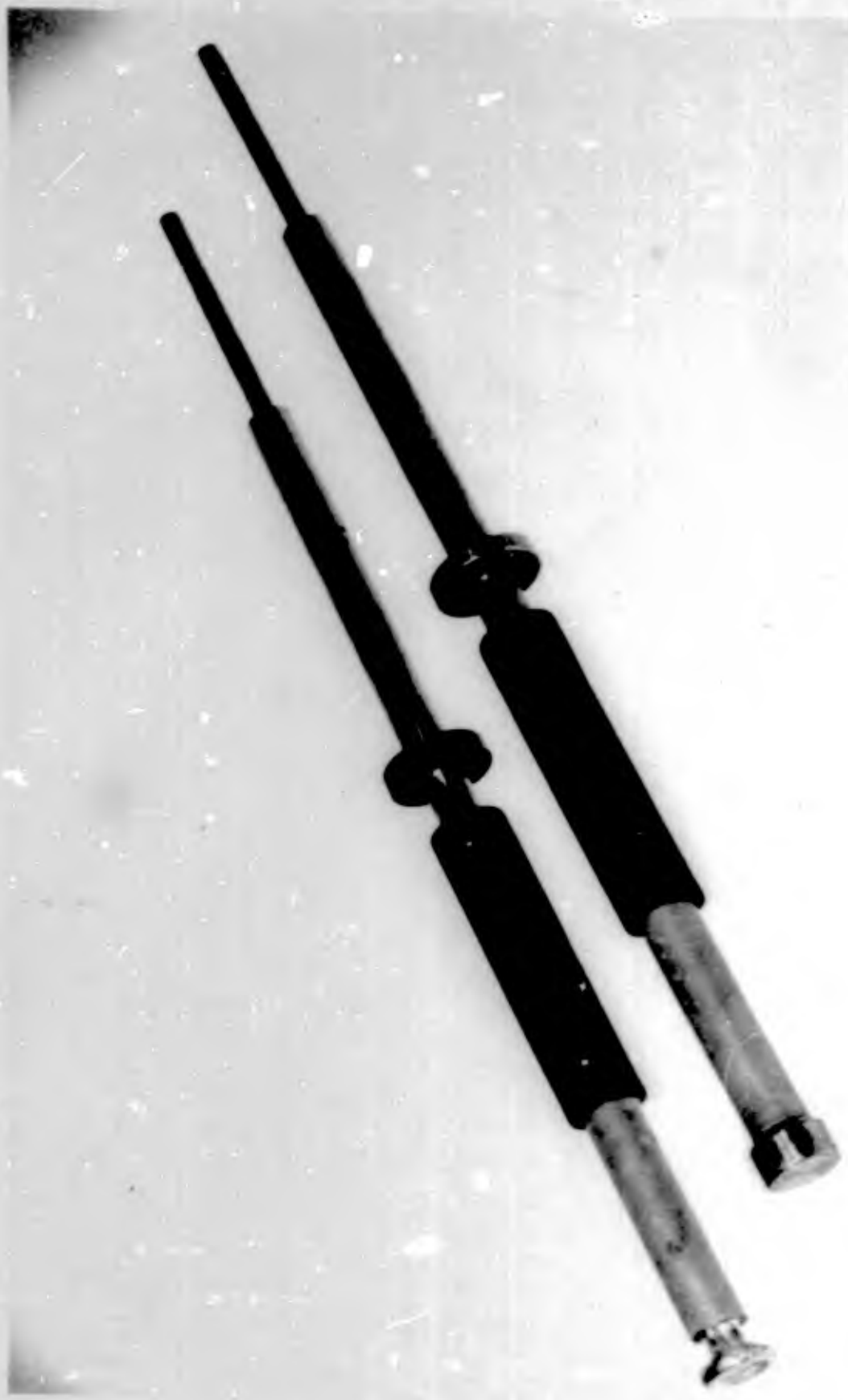

HIGH PRESSURE (8000 PSIA) ARC HEATER
CENTER ELECTRODE (CATHODE) ASSEMBLIES

R-17,206
Neg. 4927-8

FIGURE XIV-18

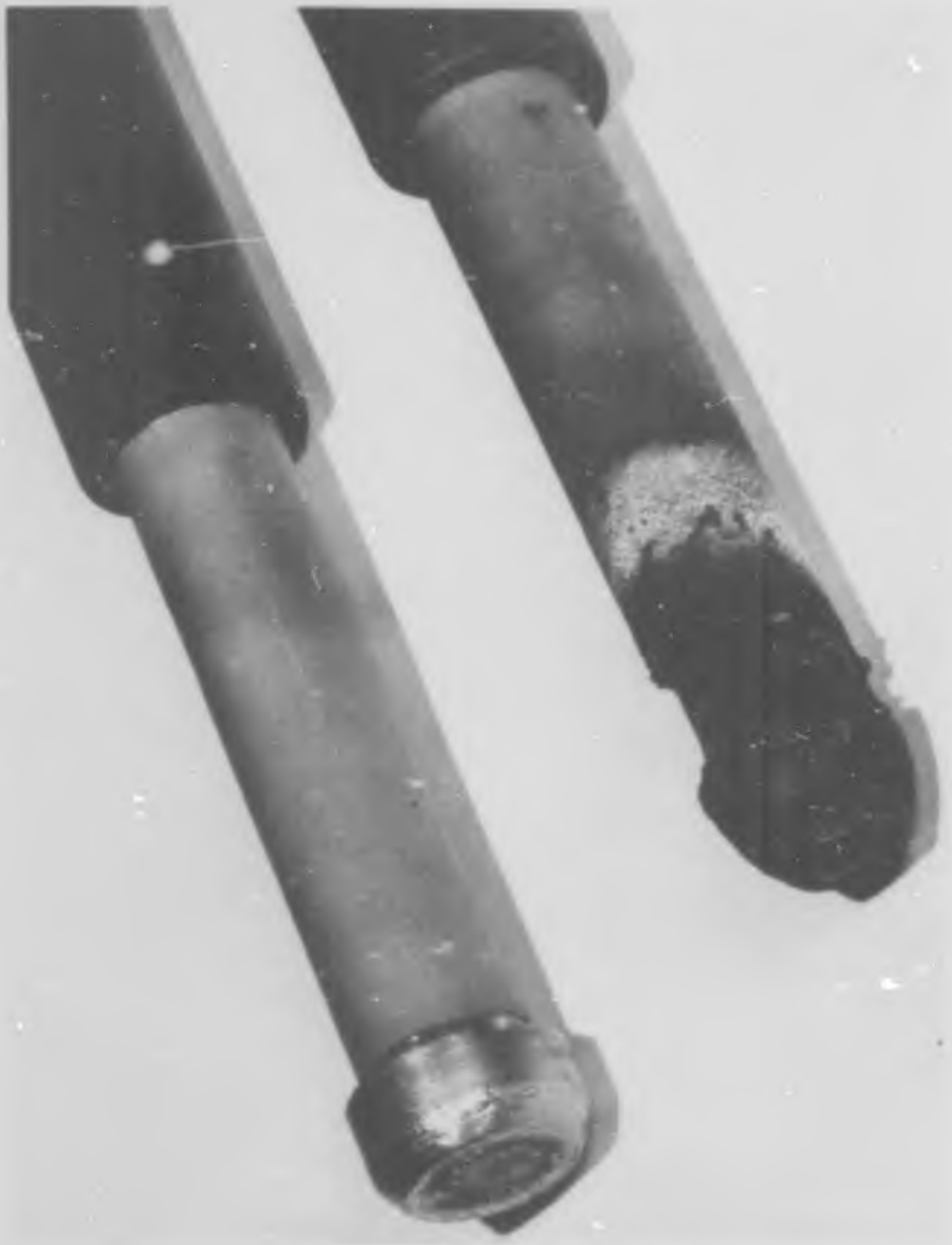

HIGH PRESSURE (8000 PSIA) ARC HEATER
CATHODE ASSEMBLIES AFTER TEST

R-17,207
Neg. T5121-4

FIGURE XIV-19

HIGH PRESSURE (8000 PSIA) ARC HEATER
CUT-AWAY CATHODE ASSEMBLIES AFTER TEST

R-17,209
Neg. T5121-5

FIGURE XIV-20

HIGH PRESSURE (8000 PSIA) ARC HEATER

FIELD STRENGTH CALIBRATION

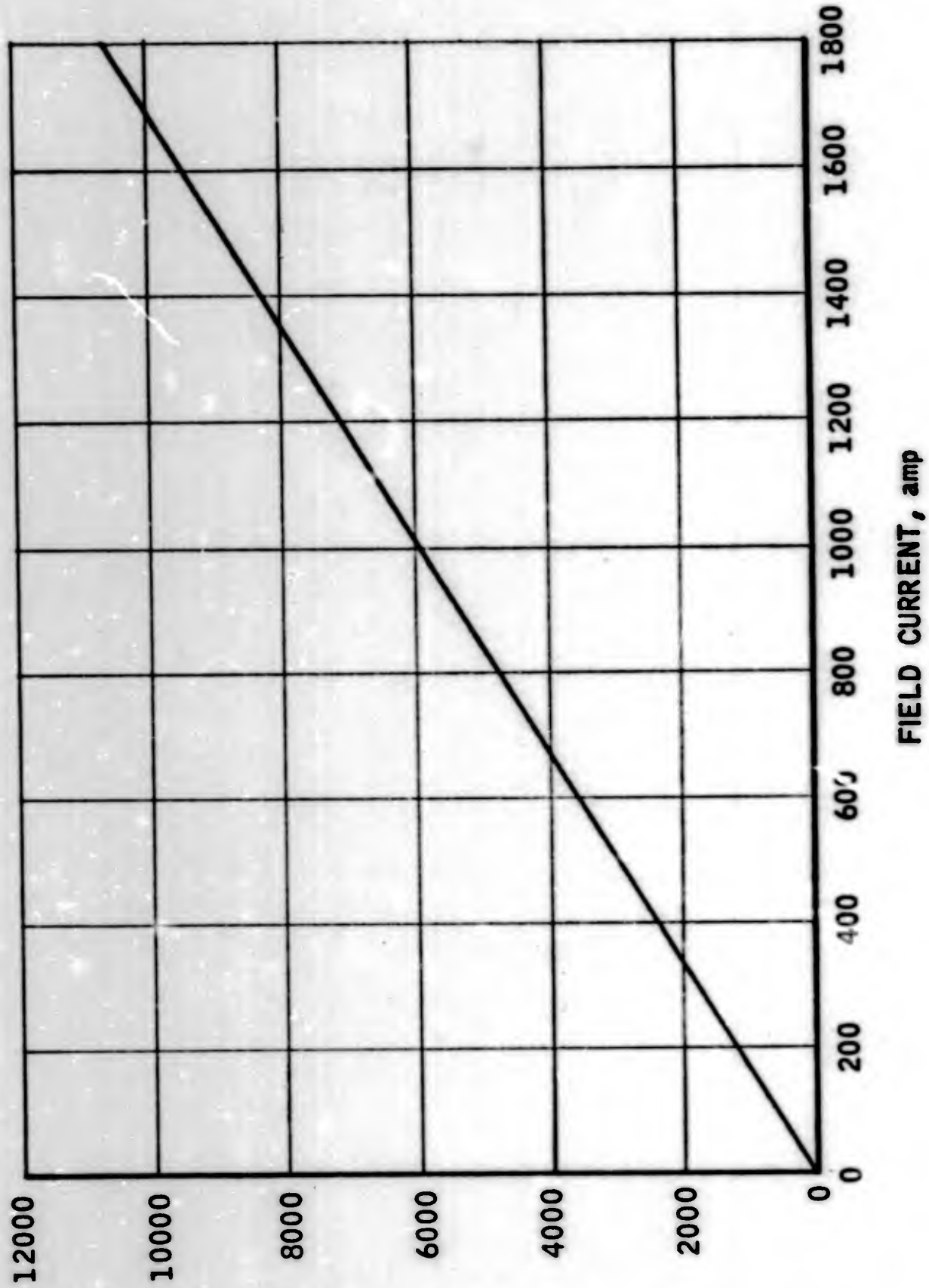

R-17,216

Figure XIV-21

b. A calibrated needle valve with micrometer adjustment for simplified inlet air metering operation.

c. An exhaust system gas cooler to reduce gas exit temperature to less than 1460°R prior to reaching the exit valve.

d. An exit gas filter to prevent graphite insulator particles from clogging the exit valve. (Filter installed following Run 1).

e. An exhaust system exit valve, which was utilized to provide a method of varying chamber pressure without physically changing the hardware. The arc heater system schematic is presented in Figure XIV-22.

f. An arc circuit ballast resistor consisting of a series of nichrome wire coils immersed in water and contained in acrylic plastic tubes as shown in Figure XIV-23. The location of the resistor in the facility circuit is shown in Figure XIV-24. The arc ballast resistor was required to limit the amount of current to the arc heater electrodes.

g. Cooling water differential temperature transducers were utilized to measure the temperature rise of the cooling water of the anode, cathode, and arc heater exit gas heat exchanger. The transducer is a 20-junction thermopile, electrically isolated, and electromagnetically shielded against any radiation fields.

5. Experiments

A total of seven runs were made during the test of the high pressure arc heater. The results are tabulated in Table XIV-II, along with pertinent remarks. The majority of the experiments were conducted with nitrogen to prolong electrode life. Run No. 6 substantiated these results with air. Maximum, steady chamber pressures of 7600 psig with nitrogen and 7400 psig with air, were achieved during arc operating times of 20 and 14 seconds, respectively.

Operational procedure of the arc heater was as follows: Initiate field coil current, set gas inlet pressure to pre-selected value, and, initiate arc. This procedure was followed to insure establishment of the field strength prior to arc initiation and to conserve the amount of gas available in the storage system. No attempt was made to obtain arc ignition at any prescribed chamber pressure. Ignition was obtained at chamber pressures ranging from 1300 psig to 5000 psig. Termination of the arc was voluntarily accomplished by tripping the main circuit breakers.

BLANK PAGE

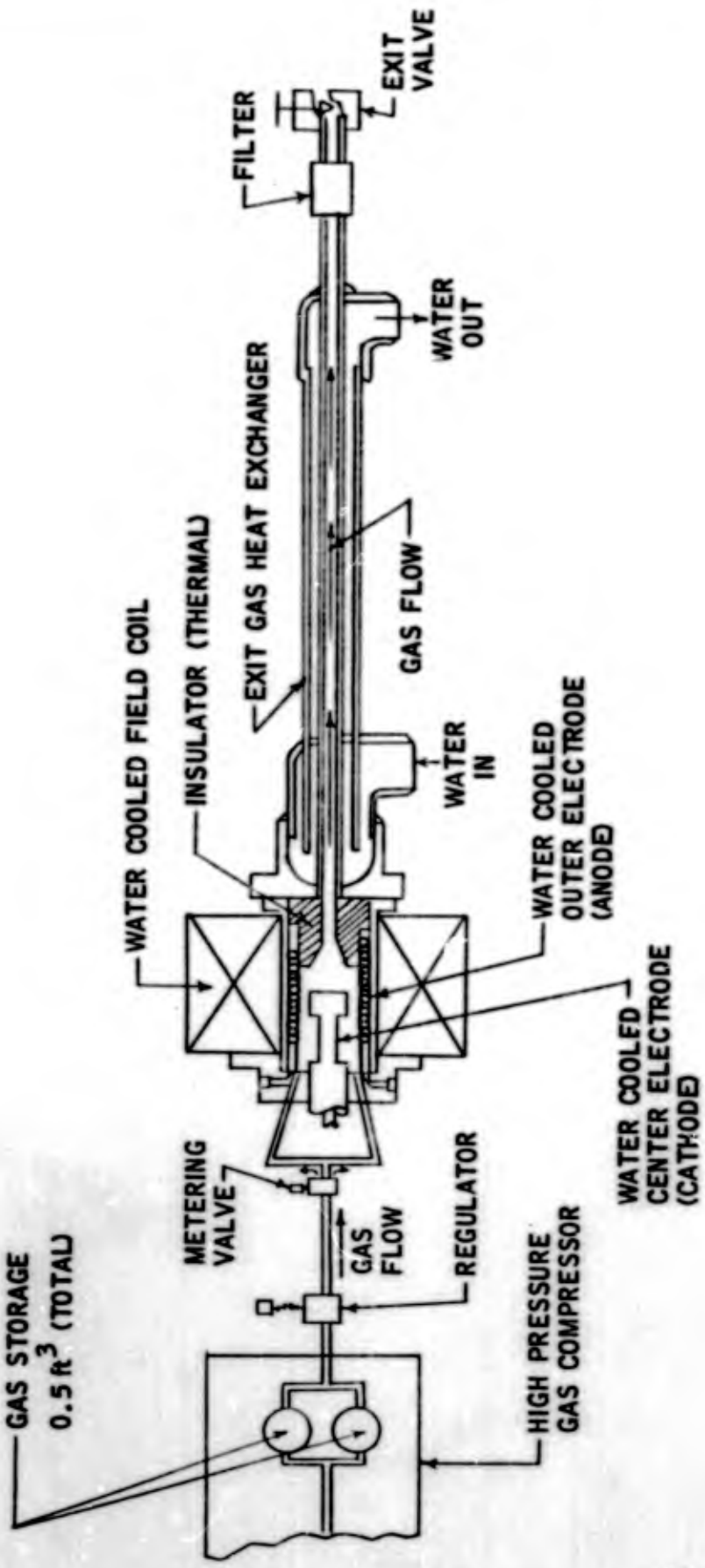

HIGH PRESSURE (8000 PSIA) ARC HEATER
SYSTEM SCHEMATIC

R-17,217

Figure XIV-22

BALLAST RESISTORS - ARC CIRCUIT

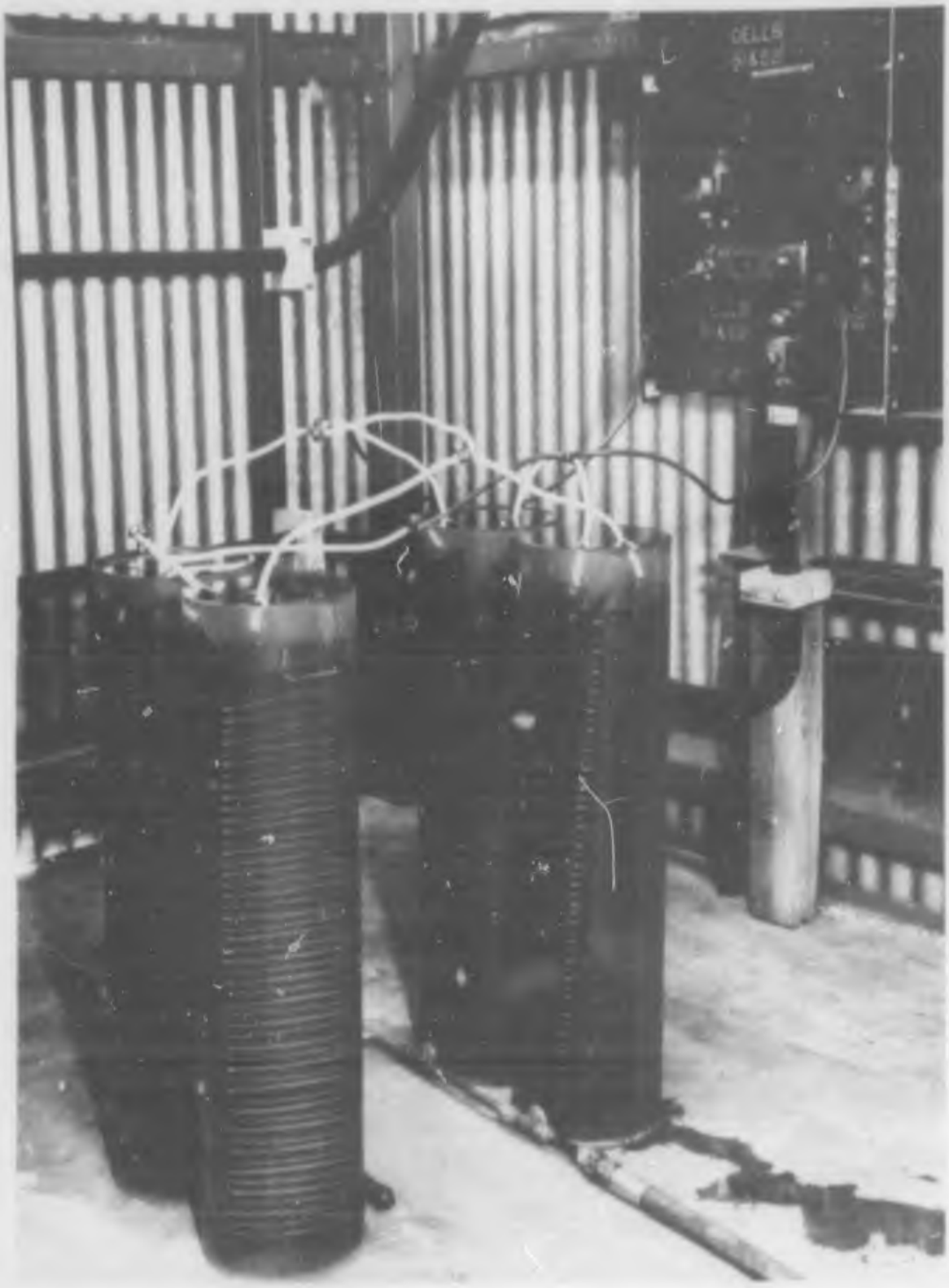

R-17,208
Neg. T5121-3

FIGURE XIV-23

FACILITY ARC CIRCUIT SCHEMATICS

CIRCUIT #1

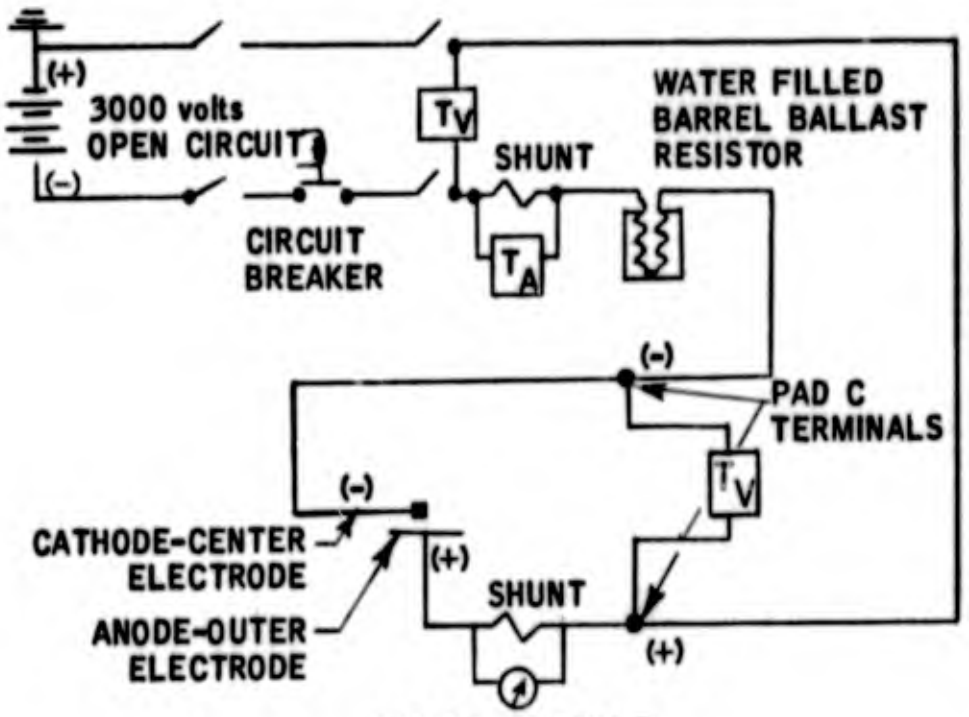

CIRCUIT #3

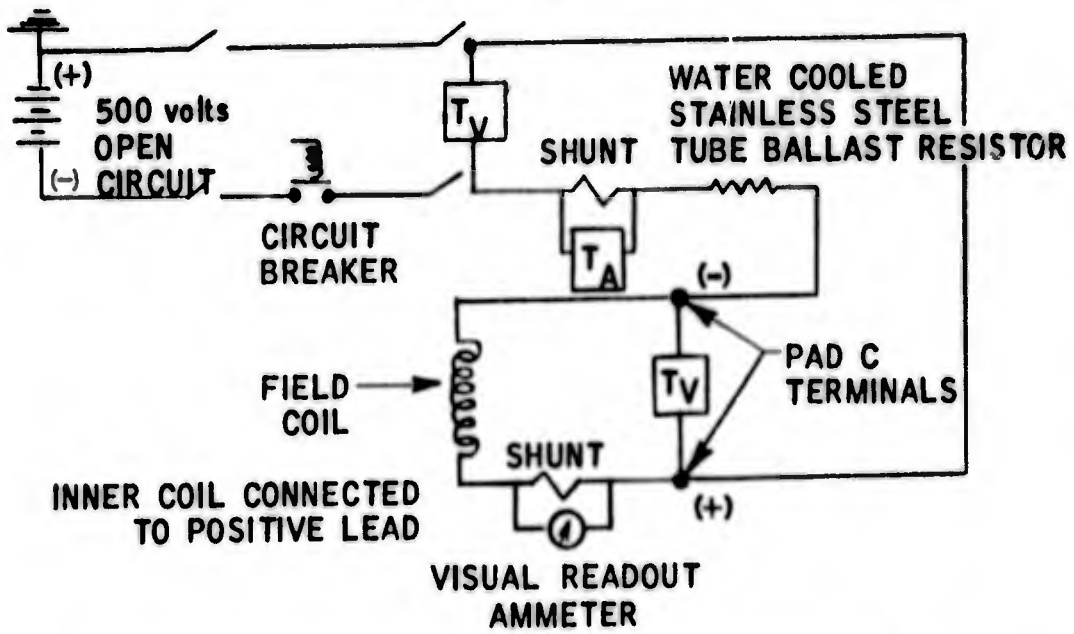

T_V - VOLTAGE TRANSDUCTOR - OUTPUT TO OSCILLOGRAPH

T_A - CURRENT TRANSDUCTOR - OUTPUT TO OSCILLOGRAPH

R-17,218

Figure XIV-24

TABLE XIV-II

SUMMARY OF TEST CONDITIONS
HIGH PRESSURE ARC HEATER

8000 psi

Run No.	Test Gas	① Gas Weight Flow (lb/sec)	Arc Gap - Nominal (in.)	Arc Time (sec)	Gas Inlet Total Pressure (psig)	Chamber Pressure (psig)	Arc Current - Nominal (amps)	Arc Voltage - Nominal (volts)	② Power to Arc - Average (Ka)	Chamber Inlet Gas Temperature (°R)	③ Chamber Inlet Gas Enthalpy (Btu/lb)	④ Power Loss to Anode (Ka)	⑤ Power Loss to Cathode (Ka)	⑥ Power Loss to Heat Exchanger (Ka)	⑦ Gas Temperature at Heat Exchanger Exit (°R)	⑧ Gas Enthalpy at Heat Exchanger Exit (Btu/lb)	⑨ Power to Gas ⑦-③x① / 0.948 (Ka)	⑩ Power to Arc from Temperature Rise Measurements ④+⑤+⑥+⑧ (Ka)	⑪ Total Power to Gas ⑥+⑧ (Ka)	⑫ Arc Heater Efficiency ⑪/⑨	Power Difference between Electrical and Temperature Power to Arc	Chamber Exit Gas Enthalpy ⑨ 0.948 + ③ (Btu/lb) ①	Chamber Exit Gas Temperature (°R)	Field Current (amps)	Field Strength (gauss)	Type Cathode	Remarks
1 *	N_2	0.049	0.1	5.2	6200	1600 ↓ 2750	260	400 ↓ 525	104 ↓ 136	-	-	-	-	-	-	-	-	-	-	-	-	-	-	1370	8,100	X6458 #1 (solid end)	Arc blowout due to high value of arc circuit ballast resistance which limited available supply voltage to arc. (Chamber pressure increase due to exit valve clogging.)
2	N_2	0.046	0.1	11.2	6200	4200	410	365	149	480	116	92.3	-	14.0	555	134	0.9	-	14.9	≈10.0	-	423	1650	1760	10,200	↓	Arc voluntarily terminated during Runs 2-6.
3	N_2	0.045	0.1	10.2	7250	5950	400	360	144	480	116	94.5	19.9	8.6	540	130	0.7	123.7	9.3	7.5	14.0	312	1250	1730	10,000	X6458 #2	
4	N_2	0.031	0.1	13.8	8200	6450	430	350	150	470	114	98.0	23.6	11.2	560	135	0.7	133.5	11.9	8.9	11.0	478	1800	1610	9,400	↓	
5	N_2	0.023	0.1	20.0	8450	7600	420	360	151	470	114	106.0	24.6	6.4	550	133	0.5	137.5	6.9	5.0	8.9	398	1550	1660	9,300		
6	Air	0.024	0.1	14.1	8400	7400	430 ↓ 400 **	315 ↓ 550 **	135	470	114	86.0 ***	25.9 ***	10.2 ***	550 ***	133 ***	0.5 ***	122.6 ***	10.7 ***	8.7	9.2	537 ***	2100	1680	9,800	↓	Excessive erosion of cathode and buildup of copper-oxide on cathode noted following run.
7 *	N_2	≈0.042	0.1	3.8	8600	4700 5000 5300	625 710 710	305 310 315	190 ↓ 220	-	-	-	-	-	-	-	-	-	-	-	-	-	-	1660	9,600	X6468 (Tubular ring end)	Investigation of arc characteristics at higher current--Severe damage to anode.

Notes: Same outer electrode (anode) used for all runs.
* Run time insufficient for steady state temperature data.
** Variation to these values during last five seconds of run.
*** Values at time = 9 seconds. Temperature data still rising slightly.

The test fluid enthalpy was calculated utilizing the measured gas temperature at the heat exchanger exit and the heat exchanger cooling water temperature rise data. The runs were, generally, continued until steady state temperature rise data were obtained.

Figures XIV-25 through XIV-28 present the variations of significant parameters with time during Runs 2, 3, 5, and 6. The increase in arc voltage during the later part of Run No. 6 is assumed to result from the erosion of the cathode (which changed the arc gap length) and the build-up of copper oxide deposits.

a. Heater Efficiency

The heater efficiencies indicated in Table XIV-II range from 5 to 9 percent. These efficiencies were calculated from the cooling water flow rates and temperature rise data of the anode, cathode, and heat exchanger and the measured gas temperature at the exit of the heat exchanger. Also shown in Table XIV-II is a comparison of the power to the arc from electrical measurements (arc voltage and arc current) and cooling water temperature data. The electrical measurements of power to the arc are consistently 10 percent higher than the power obtained from temperature data. This difference is within the accuracy of the instrumentation in addition to being in a direction to be expected since losses to the uncooled arc heater hardware (flanges, insulator, etc.) were not obtainable.

Although the arc heater efficiencies presented are relatively low, by arc heater standards, it is assumed they result from the short arc gap length ($\approx$ 0.1 inch). A larger arc gap should result in a larger arc voltage requirement (for constant arc current and chamber pressure). This would increase the total power to the arc heater without increasing the percentage losses to the anode and cathode, with a resulting increase in a percentage of the power to the gas. (The above hypothesis necessarily assumes that the anode and cathode fall regions are basically a function of the arc current, the chamber pressure, and the work function of the electrode material).

b. Heater Exit Gas Enthalpy

As shown in Figure XIV-29, the gas enthalpies obtained during this program are substantially below the extrapolated state-of-the-art curve for the 8000 psi test region. (Note, however, that the 3000 psi arc heater test data is a substantial improvement in the state-of-the-art for arc heater technology). High gas enthalpy levels were not the primary objectives for the CY 63 high pressure level

BLANK PAGE

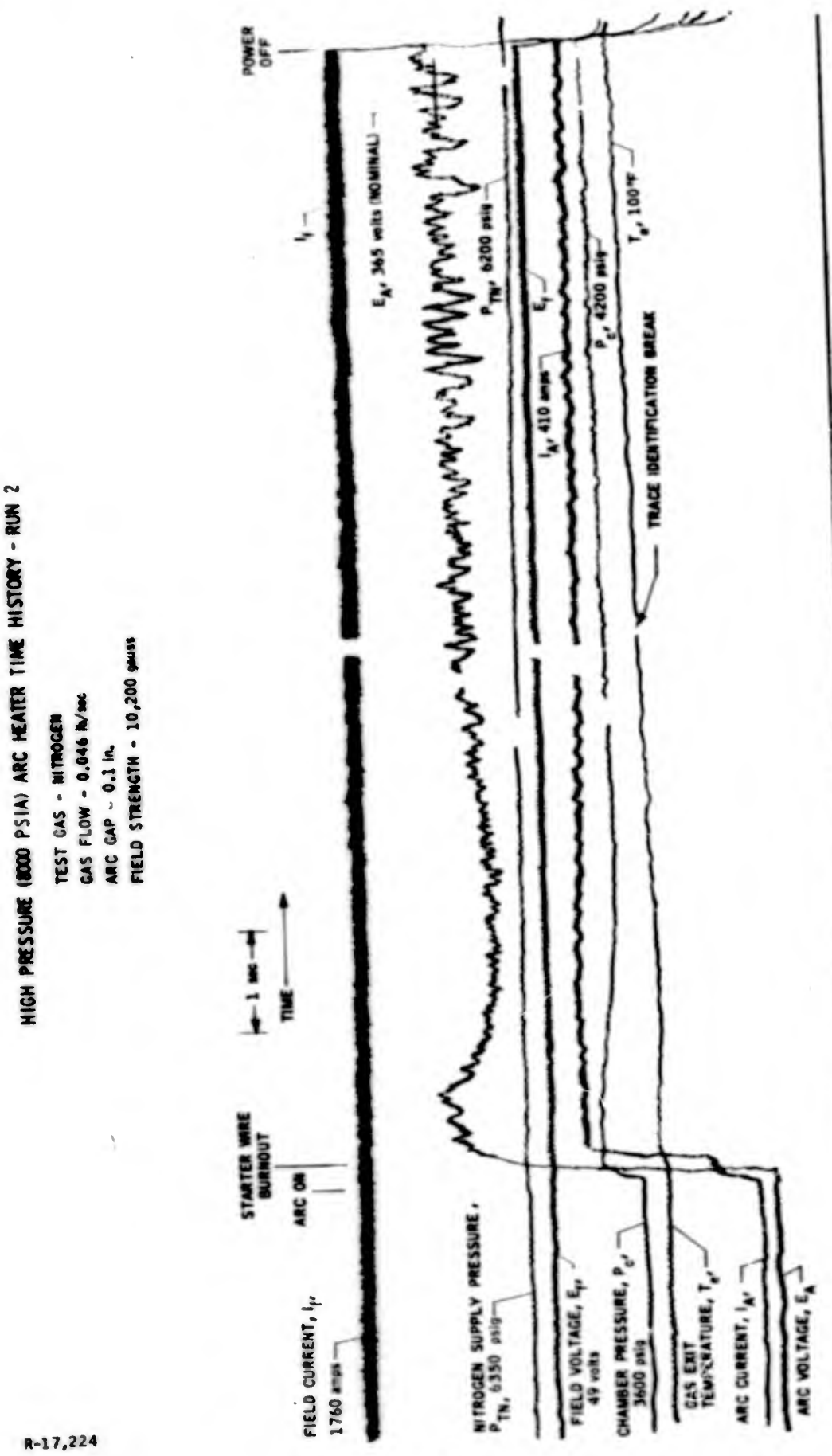

R-17,224

Figure XIV-25

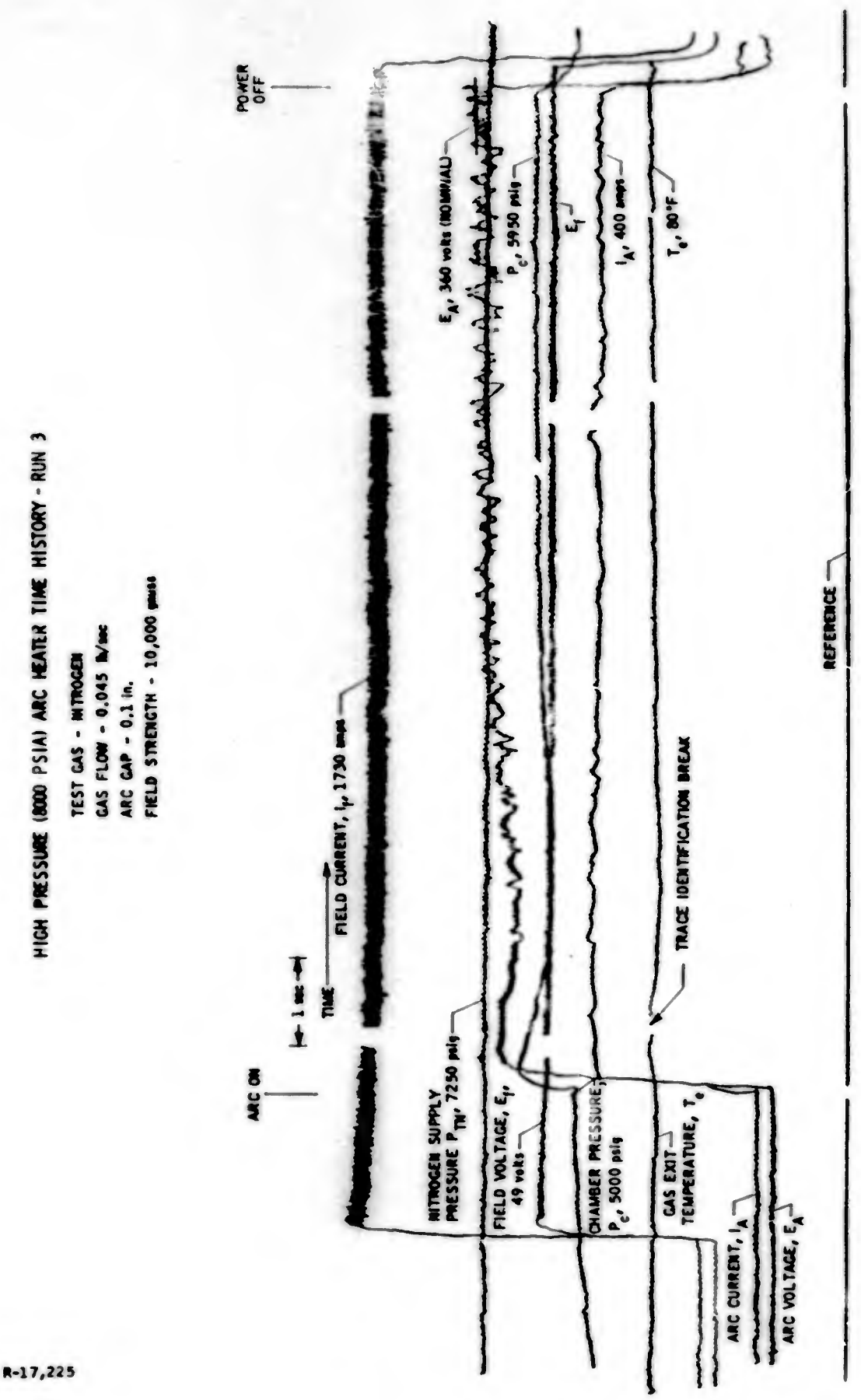

Figure XIV-26

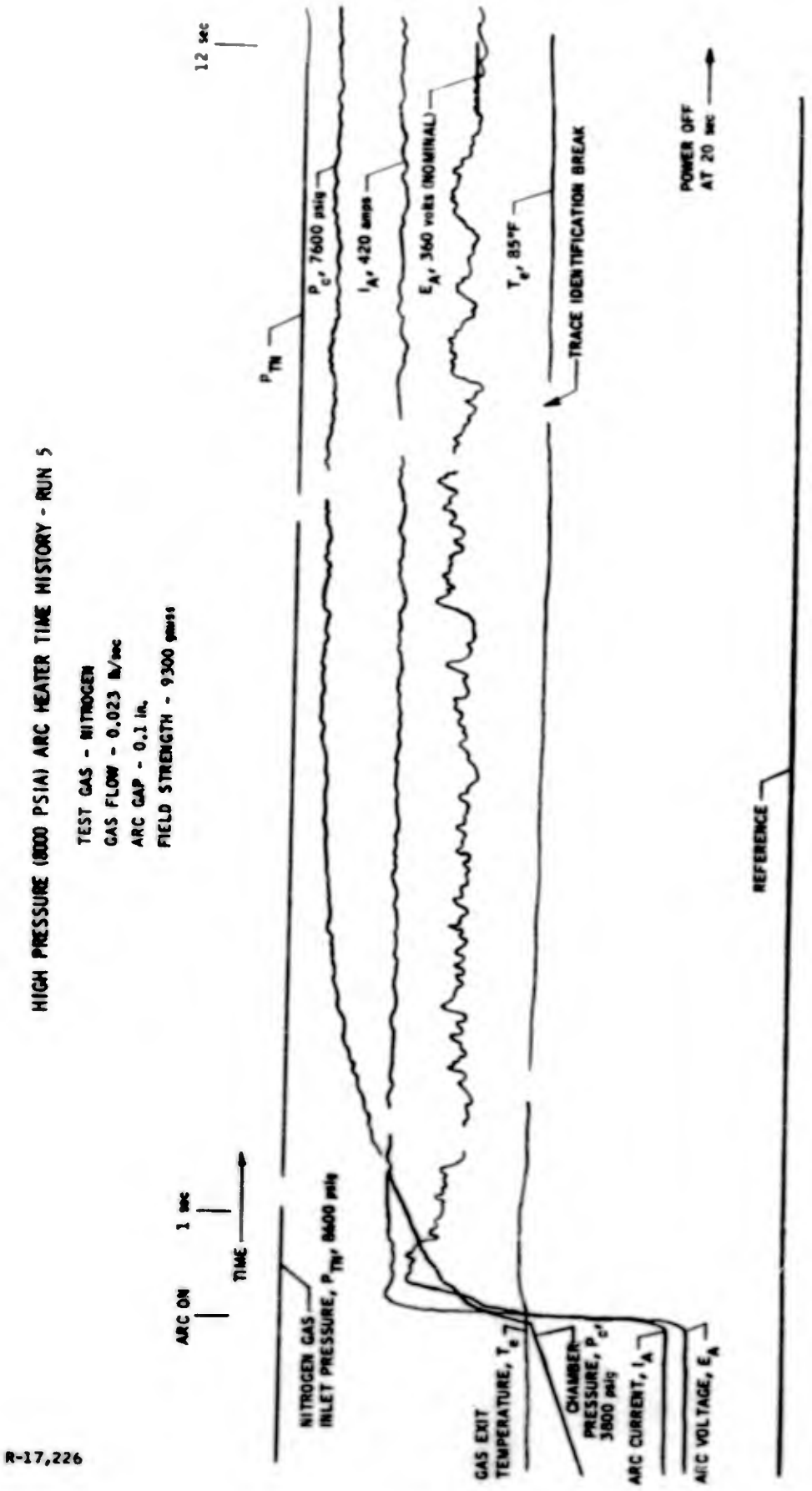

Figure XIV-27

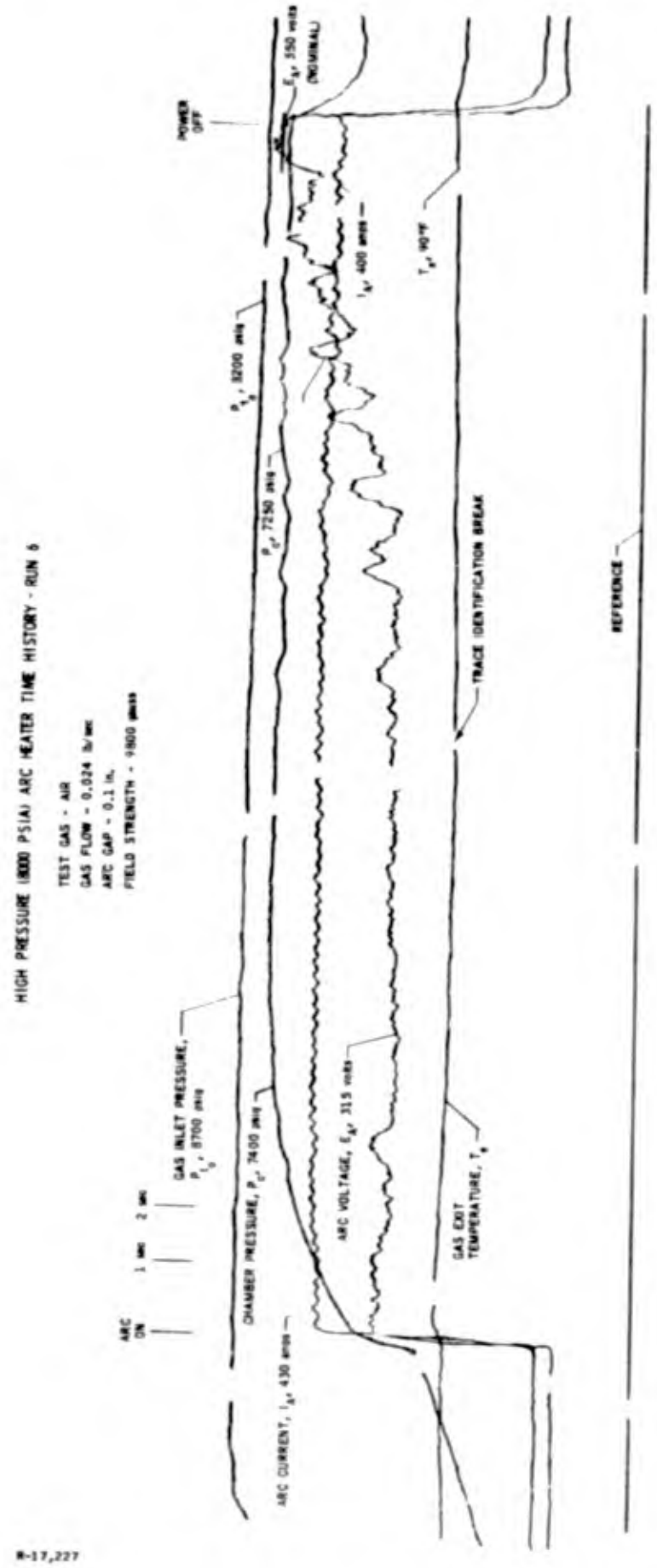

Figure XIV-28

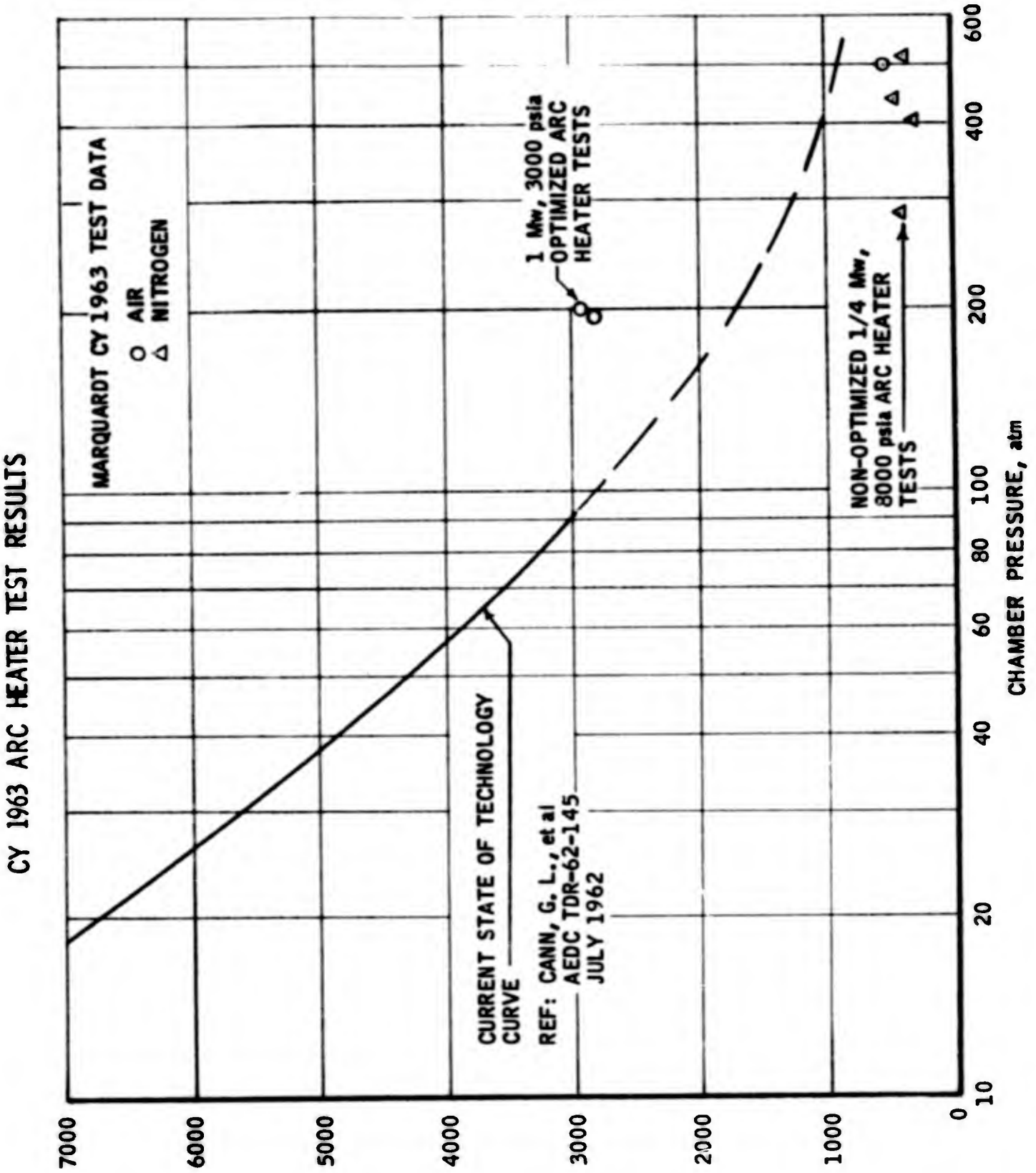

R-17,219

Figure XIV-29

arc heater experiments. The data do indicate, however, that higher gas enthalpies are possible at these high pressures by optimizing the heater geometry, reducing the gas weight flow rate, and by increasing the arc gap length.

c. Parameters of Voltage and Current

Parameters of arc current and arc voltage are presented in Figure XIV-30 for the various chamber pressure levels tested. The data show a lower arc voltage is required during operation with air than with nitrogen at similar conditions, a trend previously indicated with other Marquardt high pressure arc heaters. This trend is generally assumed to result from the lower ionization of oxygen as compared to nitrogen voltage requirements.

d. Pressure

Sufficient runs were not available to accurately determine the effect of pressure on required arc voltage, since for the runs shown in Figure XIV-29 an additional parameter, gas flow, varied from run to run. However, in comparing selective runs (2 and 3) in the range of 4000 to 6000 psig, the pressure appeared to have little effect on required arc voltage.

e. Arc Gap

The arc gap length of 0.1 inches utilized during this program was nominally the same as the gap used during CY 1962 when arc operation at high chamber pressures was obtained. The effect of arc gap length on arc heater performance was not investigated during this program.

f. Magnetic Field

The effect of magnetic field strength upon arc voltage requirements was not determined during this experimental program. Excellent arc heater operation was obtained for the field strengths of 9300 to 10,000 gauss utilized during this program.

D. Results and Conclusions

The CY 63 Arc Heater test programs were successfully completed, extending the capability of full simulation over a greater portion of the flight spectrum than heretofore possible. The analytical studies completed indicate that a supersonic arc heater is feasible, and may extend the capabilities of arc heaters past the limits presently encountered with conventional subsonic units.

HIGH PRESSURE (8000 PSIA) ARC HEATER

SYMBOL	RUN	CHAMBER PRESSURE, psig	GAS FLOW, lb/sec	TEST GAS
○	1	~2750	0.049	N_2
△	2	4200	0.046	N_2
□	3	5950	0.045	N_2
◇	4	6450	0.031	N_2
▽	5	7600	0.023	N_2
D	7	4700	~0.042	N_2
D	7	5000	~0.042	N_2
D	7	5300	~0.042	N_2
●	6	7400	0.024	Air

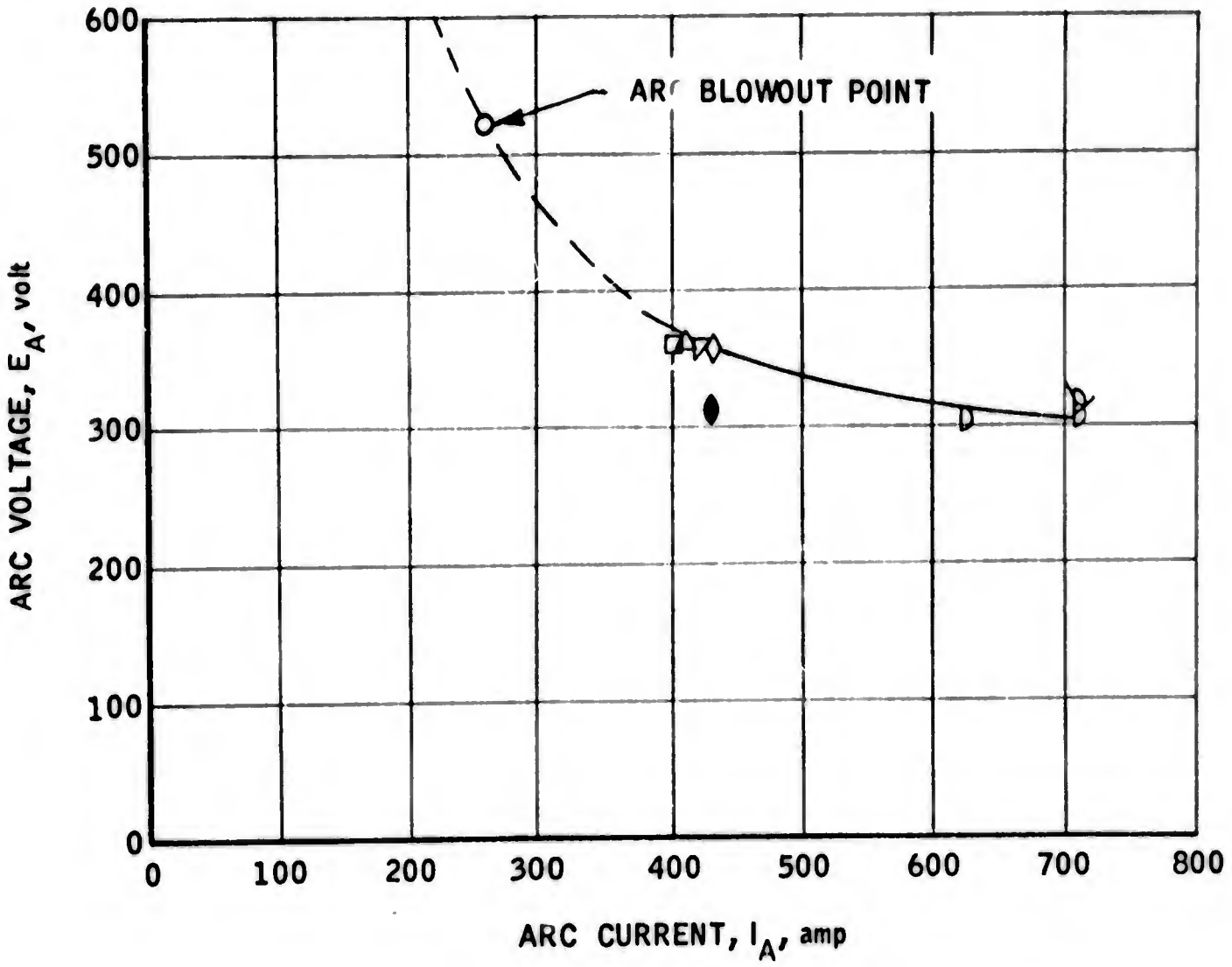

The development and testing of the 3000 psi, 1 Mw arc heater was successfully completed by meeting the design goals. Successful operation was realized at a pressure of 2800 psia, at a power level of 1.12 Mw, and an enthalpy addition to the air of 3150 Btu/lb. The maximum operating pressure, in the flow range involved, was limited only by the supply storage pressure (3000 psi max.) and the pressure losses in the lines due to flow. The reader is again referenced to Figure XIV-29 for an indication of the arc heater state-of-the-art extension by this heater.

Development and testing of the 8000 psi, ¼ Mw Arc Heater was successfully completed with the operation of an arc heater with air at a pressure of 7400 psia and nitrogen at 7600 psia at a power level of approximately 150 Kw. It was considered that enthalpy levels higher than demonstrated are possible by optimizing the arc heater design, reducing the gas flow rate, and by increasing the arc gap length.

XV. HIGH PRESSURE AIR GENERATION RESEARCH

Extremely high pressure air is necessary for research studies associated with airbreathing propulsion system experiments that require simulated flight environments in the high speed regions of the air-breathing flight corridor. Limitations of air compressors have generally been exceeded by facility requirements for ultra high pressure air. The high air-flow rates, coupled with the ultra high pressure requirements, has somewhat narrowed air supply system concepts to a blowdown simulation system that must be periodically regenerated.

Studies conducted under the CY 1962 Air Force - Marquardt Contributing Engineering Program (Reference XV-1) successfully reached pressures in excess of 40,000 psia utilizing the principle of heating a cryogenic fluid in a constant volume vessel. The test pressure vessel used during CY 1962 was also used to conduct the CY 1963 Ramjet Technology experiments using both liquid nitrogen and liquid air. In addition to demonstrating the pressure level attainable, pressure, specific volume, and temperature (PVT) data were obtained for air at pressures far above currently available information.

The maximum pressure level attained under this program was 62,800 psia, at a fluid temperature of 790°R. Air PVT data was obtained for a specific volume range of 0.0182 to 0.0264 lb/ft^3.

A. Test Equipment

The experiment utilized a pressure vessel, constructed under the CY 1962 Contributing Engineering Program (Contract AF 33(600)-40809), of Vascomax 300 CVM high strength 18 percent maraging steel designed to withstand a pressure of 100,000 psi. Photographs of the high pressure vessel are presented in Figures XV-1 and XV-2.

In order to create the extremely high pressures, it was necessary to submerge the vessel in silicon oil and heat the vessel and oil with a coil heater element. Figure XV-3 shows the vessel installed in the oil container. Silicon oil was utilized because of its high temperature properties. The heater element consists of four, 8 inch diameter coils of nichrome wire with magnesium oxide insulation and an incoloy sheath, rated at 1500 watts with a supply voltage of 200 volts.

- -

REFERENCE XV-1 Cox, P. B. "Phase I Summary Technical Report on the CY 1962 Air Force - Marquardt Contributing Engineering Report". Report 25,065 Volume VII, February 1963 UNCLASSIFIED

HIGH PRESSURE AIR GENERATION SYSTEM COMPONENTS

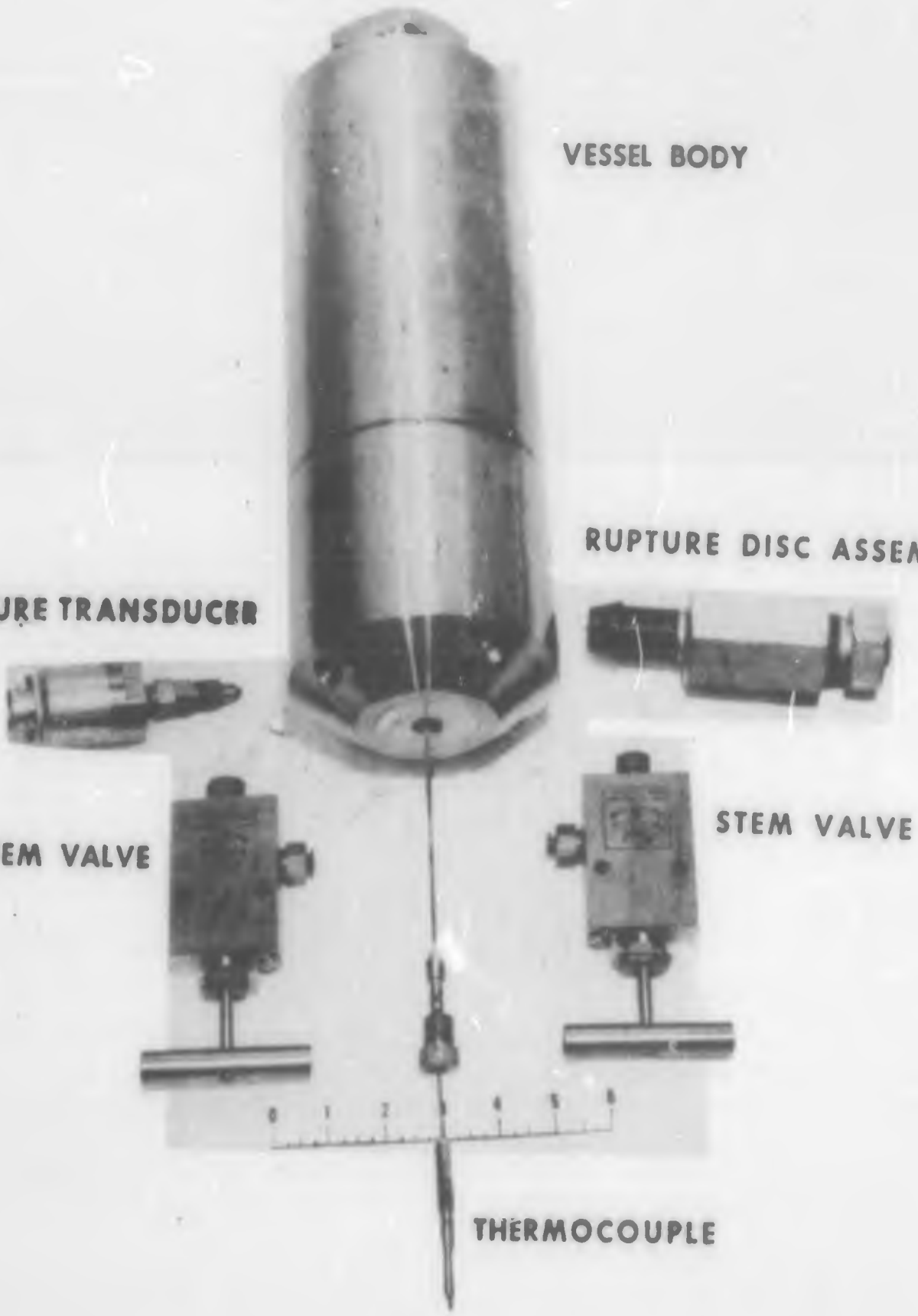

R-12,649

FIGURE XV-1

BLANK PAGE

HIGH PRESSURE AIR GENERATION VESSEL COMPONENTS

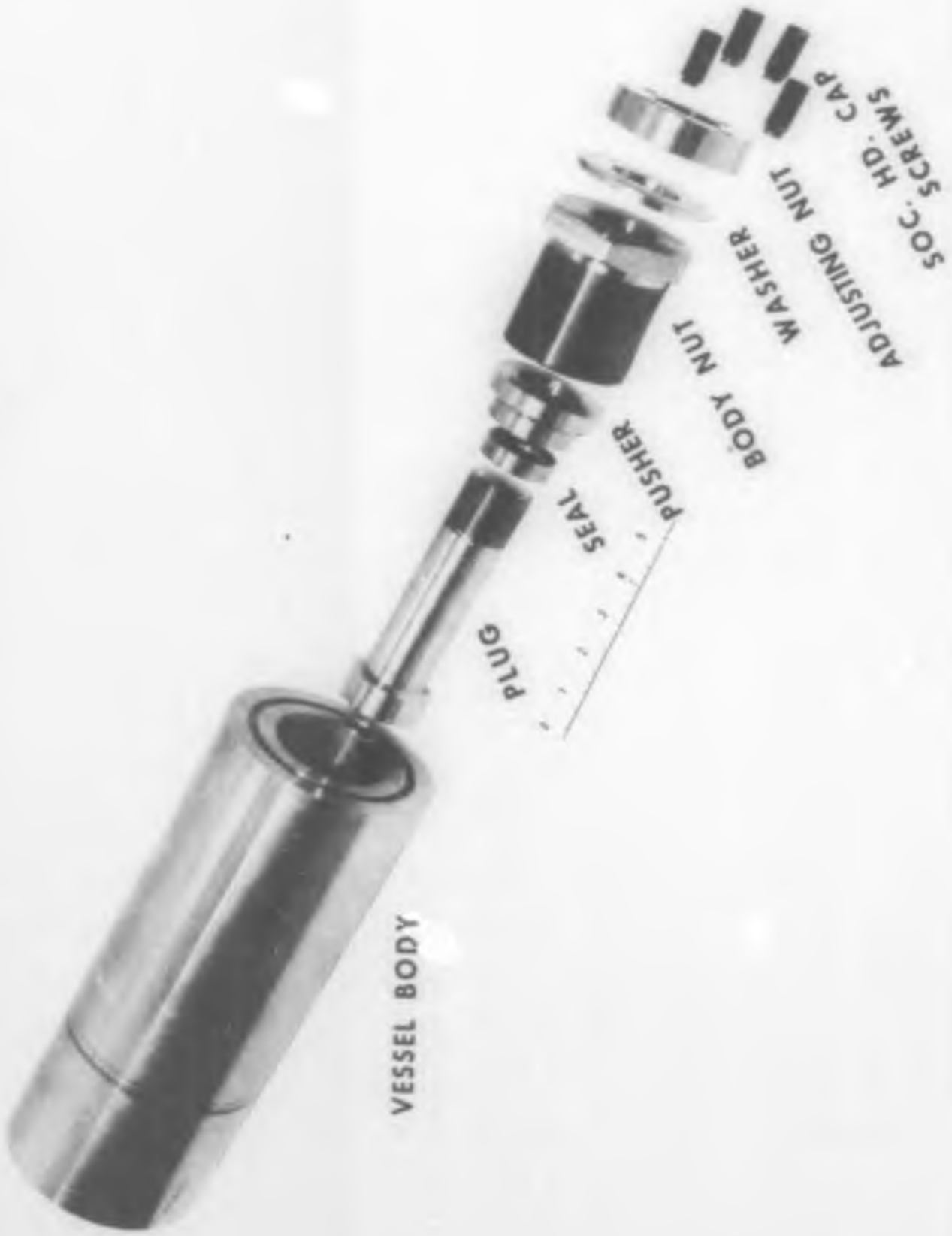

R-12,648

FIGURE XV-2

HIGH PRESSURE AIR GENERATION VESSEL SUBMERGED IN OIL

R-17,265
Neg. T5114-3

FIGURE XV-3

A heat-up time of approximately 3 hours was required to reach the maximum temperature (~860°R) of the system. This upper limit was due to heat losses of the oil to the atmosphere. Figure XV-4 is a photograph of the vessel and associated equipment installed at the test site.

The system also incorporated a technique for measuring the weight of air in the high pressure vessel in order to determine the density at various vessel fill levels. The weight measuring system, shown in Figure XV-4, consists of a low pressure chamber of known volume (1394 in^3) equipped with pressure and temperature instrumentation. The volume of the low pressure chamber was determined by three methods. (1) Calculated volume from dimensions, (2) Difference in chamber weight when filled with water and empty and, (3) Measured volume obtained by filling chamber with water and measuring the amount of water contained in the chamber. The percentage difference between the average value and the minimum and maximum value obtained by the three methods was ± 0.32 percent. The density of the liquid in the high pressure vessel was determined by expanding the high pressure vessel fluid into the low pressure chamber at the completion of the test run. Since the initial and final conditions in the low pressure chamber were measured, the initial weight of air in the high pressure vessel can be calculated from perfect gas relationships. The regime is such that the relations are perfectly valid. A schematic of the high pressure air generation system is shown in Figure XV-5.

The data recording equipment utilized consisted of the following:

1. Vessel Fluid Temperature

The output of the copper-constantan vessel thermocouple was recorded on Brown millivolt recorder.

2. Vessel Fluid Pressure

The output from the Micro-Systems pressure transducer was indicated (in terms of pressure) on the visual meter included in the Wee-Mite recorder circuit.

B. Estimated Accuracy of Measurements

The following presents the estimated accuracy of the various measurements made during the tests:

1. Vessel fluid pressure - A calibration curve of the pressure transducer and the readout unit is shown in Figure XV-6. This curve was furnished with the equipment and is certified to be within 1 percent tolerance over the range from 0-100,000 psia. Periodic calibration checks of the electrical output were made over the range of 0-10,000 psia (the maximum pressure limit of the dead weight tester available at TMC). It was found that the accuracy was well within 1 percent reading over this range.

BLANK PAGE

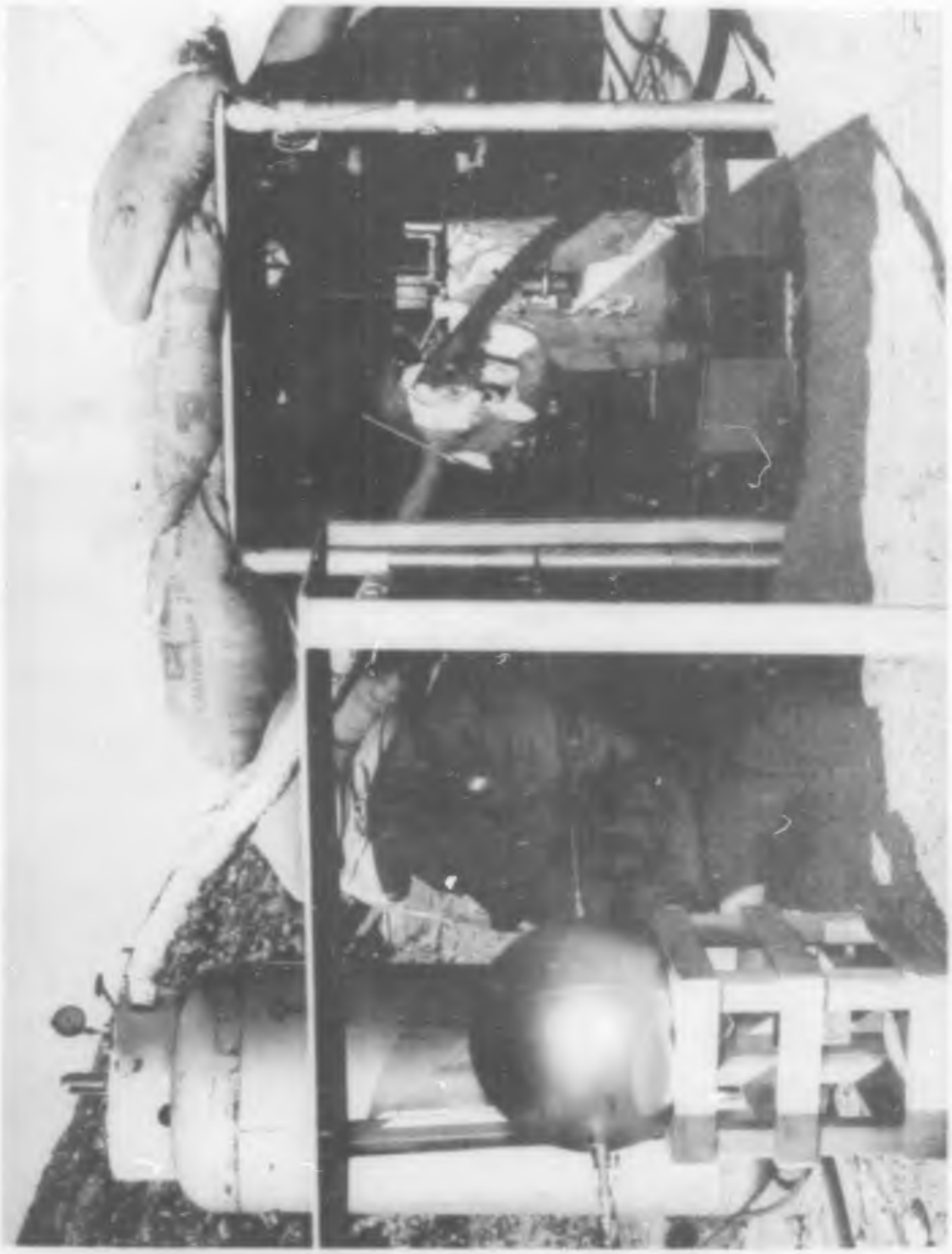

HIGH PRESSURE AIR GENERATION TEST SETUP

R-17,266
Neg. T5114-2

FIGURE XV-A

HIGH PRESSURE AIR GENERATION TEST SETUP

P_1 = VESSEL PRESSURE
P_2 = EXPANSION TANK PRESSURE
T_1 = VESSEL INTERNAL TEMPERATURE
T_2 = OIL BATH TEMPERATURE AT VESSEL
T_3 = OIL CONTAINER INTERNAL WALL TEMPERATURE
T_4 = EXPANSION TANK INTERNAL TEMPERATURE

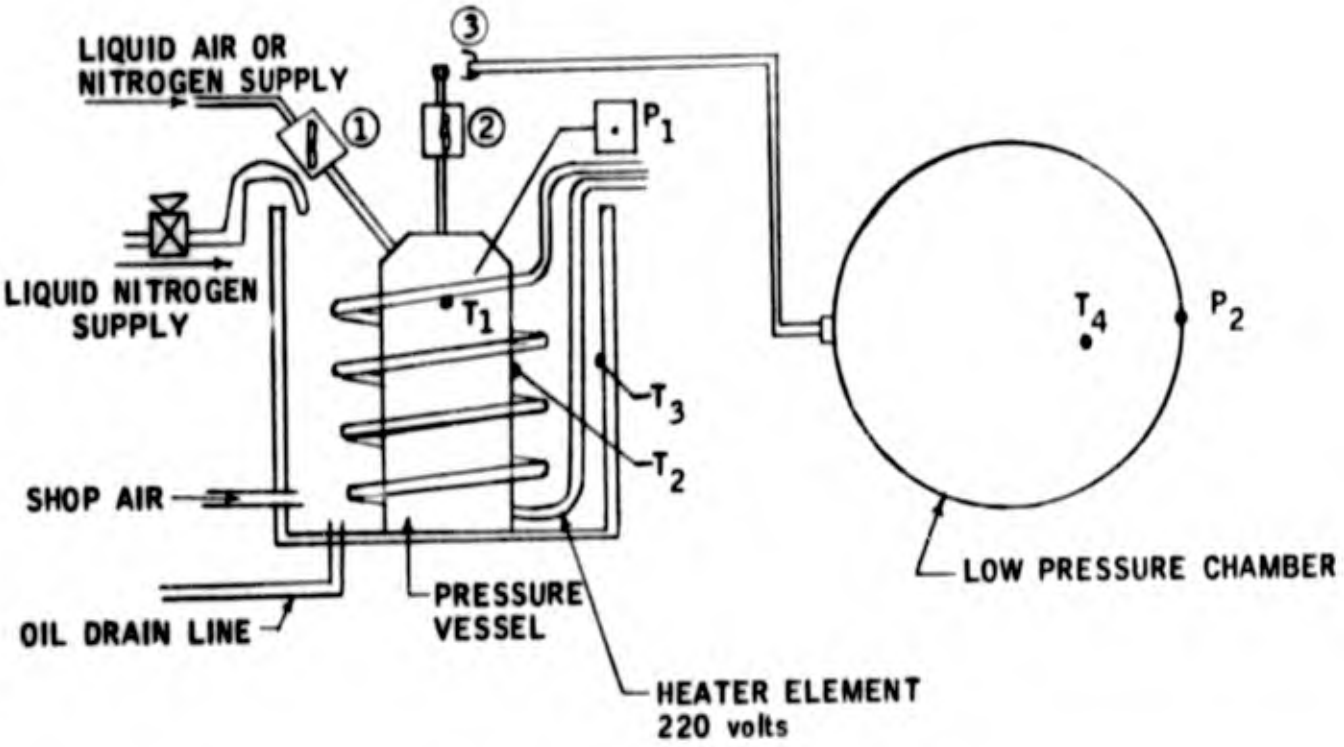

① INLET VALVE
② BLEED VALVE
③ CONNECTION TO BLEED CHAMBER MADE AFTER VESSEL IS FILLED WITH LIQUID

R-17,269

Figure XV-5

PRESSURE TRANSDUCER AND READOUT UNIT CALIBRATION DATA

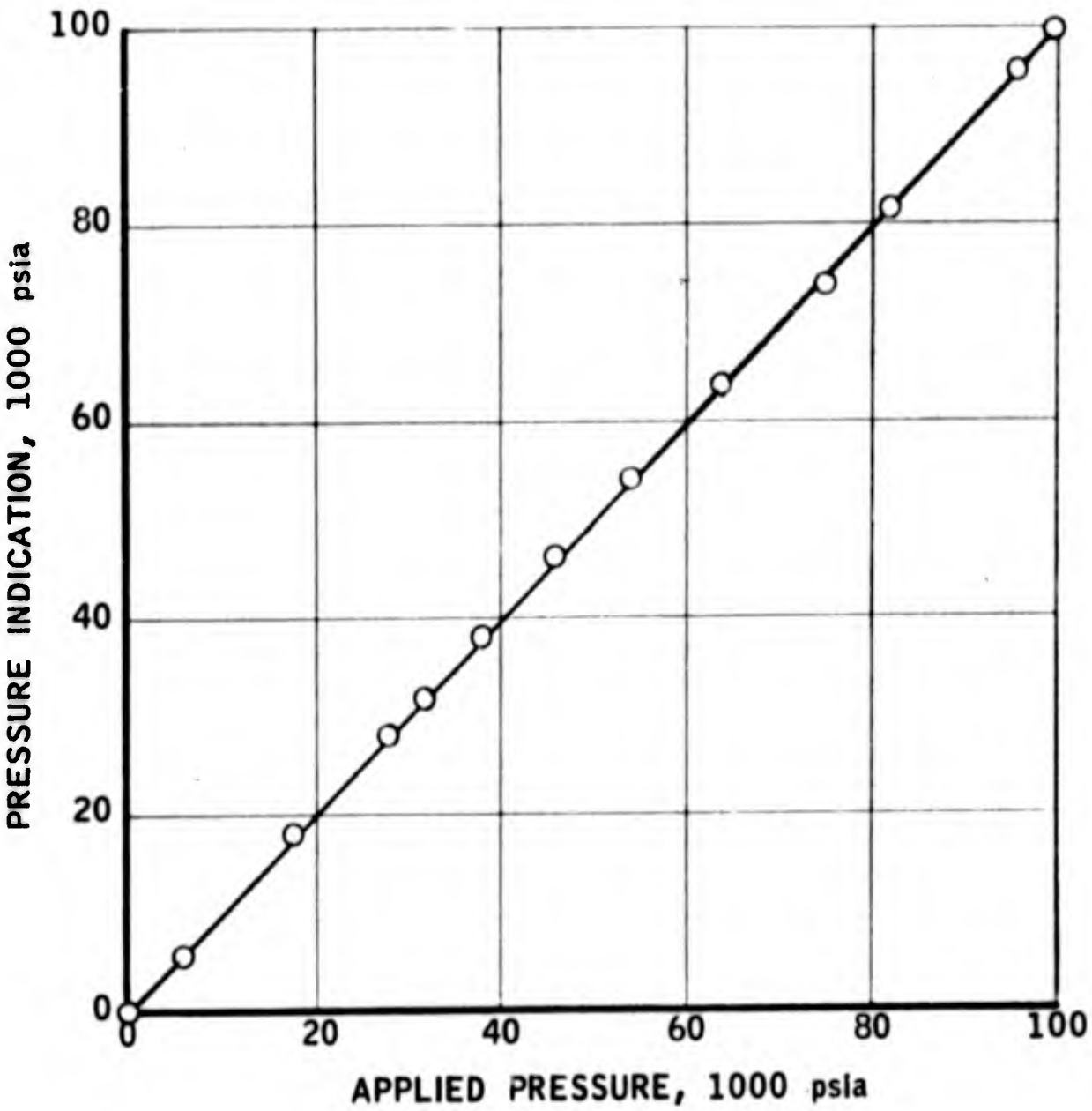

R-18,127

FIGURE XV-6

2. Vessel Fluid Temperature - Figure XV-7 presents the output of the thermocouple versus temperature. Actual calibrated points are shown. From this information the accuracy of the temperature recording system is estimated to be better than 1 percent of reading.

3. Vessel fluid density calculations based upon the pressure and temperature measurements of the low pressure chamber were estimated to have 1 percent accuracy.

C. Experimental Program

A total of 25 experimental tests were conducted with the high pressure air generation unit located at The Marquardt Research Field Laboratory located at Saugus, California. The maximum pressure attained was 62,800 psia during test Run No. 17. Table XV-I summarizes the maximum vessel fluid pressure and temperature and the difficulties, if any, that were encountered during the experimental tests. During the initial tests (Runs 1 through 12) a repeated pressure leak at one of the vessel ports precluded attainment of ultra high pressures and PVT data. Following various attempts to obtain a pressure seal, it was determined that a crack existed in the cone seat of the vessel port. This was repaired by increasing the depth of the port and re-machining the cone seat at the bottom of the port.

During Runs 15 through 17 a double junction in the vessel thermocouple precluded attainment of PVT data. Following fabrication of a new thermocouple, test runs were made at various vessel fill levels and PVT data were obtained to pressures of 50,000 psia. This limitation of 50,000 psia was imposed following Run 17 because the gland nut at the vessel from the transducer line started leaking at 62,000 psia. (A leak during a test run precludes attainment of necessary measurements required to compute the weight of fluid in the vessel and therefore, PVT data.) The leak was attributed to an incompatibility in the coefficient of expansion between the vessel port threads and the gland nut threads even though the coefficients of expansion of the material were estimated to be satisfactory.

Subsequent to the test runs where PVT data were obtained (Runs 20 through 22) leaks developed at the inlet valve line gland nut at the vessel. The tests were discontinued when the leak could not be stopped by cleaning the cone seat area and re-tightening the gland nut. The occurrence of a leak was easily recognized since a continuous plot of the data was made during the run and at various times during the run, conditions were allowed to stabilize. When a leak was present the pressure would immediately decrease.

D. Test Data

Figure XV-8 presents the data obtained at various specific

BLANK PAGE

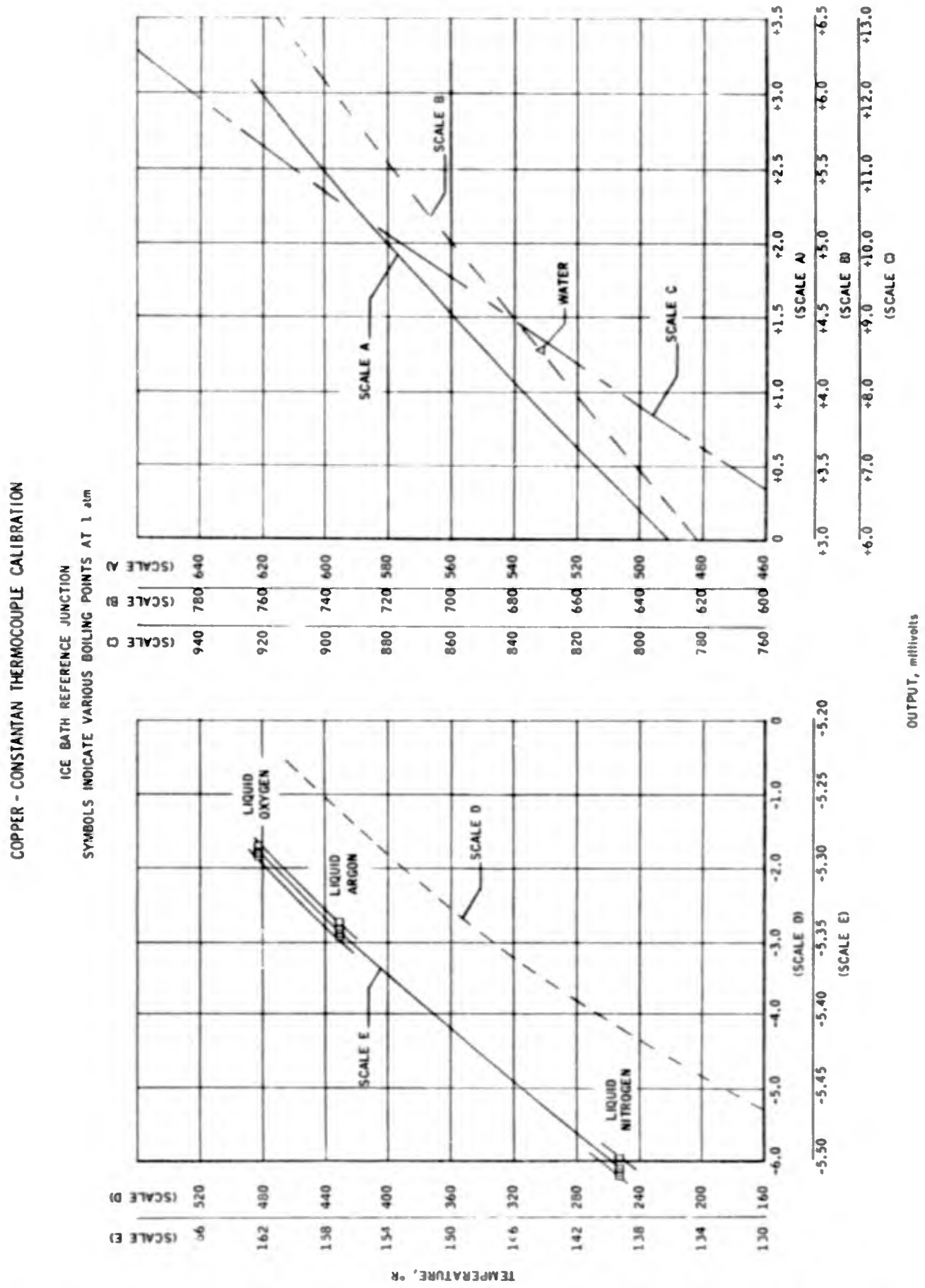

R-15,088A

Figure XV-7

TABLE XV-I

HIGH PRESSURE AIR GENERATION TEST SUMMARY

Test No.	Test Fluid	Max. Vessel Fluid Pressure psia	Max. Vessel Fluid Temperature °R	Remarks
1	Nitrogen	39,750	654	Leak in vessel thermocouple stem (thermocouple repaired).
2	Nitrogen	34,950	499	Leak at thermocouple seat (line collar adjusted and gland nut tightened).
3	Nitrogen	46,750	691	Leak at vessel on transducer line during Runs 3-7 (adjusted collar on line and tightened gland nut).
4	Nitrogen	29,250	462	Attempts to obtain seal were unsuccessful.
5	Nitrogen	27,000	440	Attempts to obtain seal were unsuccessful.
6	Air	48,400*	665	Following Run 6, new lines were installed on the transducer and burst diaphragm.
7	Air	25,000	394	Leak at transducer line at vessel.
8	Air	24,200	373	Leak still present at the vessel port of the transducer line during Runs 8-12.
9	Air	20,000	320	Cleaned transducer line vessel seat and re-installed line. Increased torque on gland nut.
10	Air	18,800	313	Leak at transducer line.
11	Air	22,300	343	Installed plug fitting at vessel transducer line port following Run 10.
12	Air	19,600	328	Installed shim on cone seat of plug fitting prior to Run 12.
				The vessel was returned to the vendor. The vessel seat is to be magnafluxed and X-rayed to determine if a crack has developed in the vessel.
13	Air			Test stopped due to erratic readings of pressure recorder. (Recorder inspected, cleaned and adjusted.) Vessel thermocouple inoperative during Runs 13 and 14.
14	Air			Leak at inlet valve. (Valve seat cleaned and refaced.)

*Zero shift in instrumentation of 1500 psia, recorded pressure, 49,900 psia.

TABLE XV-I (Continued)

Test No.	Test Fluid	Percent Oxygen	Max. Vessel Fluid Pressure psia	$\bar{v}$ cc/mole	$\bar{v}$ ft^3/lb	Max. Vessel Fluid Temperature °R	Remarks
15	Air	22	41,300			766	New thermocouple installed. Erratic temperature readings during 15-18 resulting from double junction in the thermocouple.
16	Air	22	36,000			476	Leak at transducer line gland nut.
17	Air	23	62,800			790	Max. pressure run. Leak developed at vessel gland nut, attributed to thermal expansion difference of vessel and gland nut.
18	Air	23	51300			671	Run made to check pressure seal at high pressure. 50,000 held for 1 hour.
19	Air	24	52,000	33.1	0.0182	630	PVT data run.
20	Air	22	50,800	36	0.0199	803	PVT data run.
21	Air	23	25,200	47.8	0.0264	836	PVT data run.
22	Air	22	46,900	38.0	0.021	876	PVT data run.
23	Air	22	49,100		-	763	Leak at vessel gland nut.
24	Air	25	16,300		-	504	Leak at vessel gland nut.
25	Air	32	42,200		0.0179	504	Investigation of oxygen percentage effect on pressure-versus-temperature. Leak at 42,000, pressure immediately bled to mass measuring system.

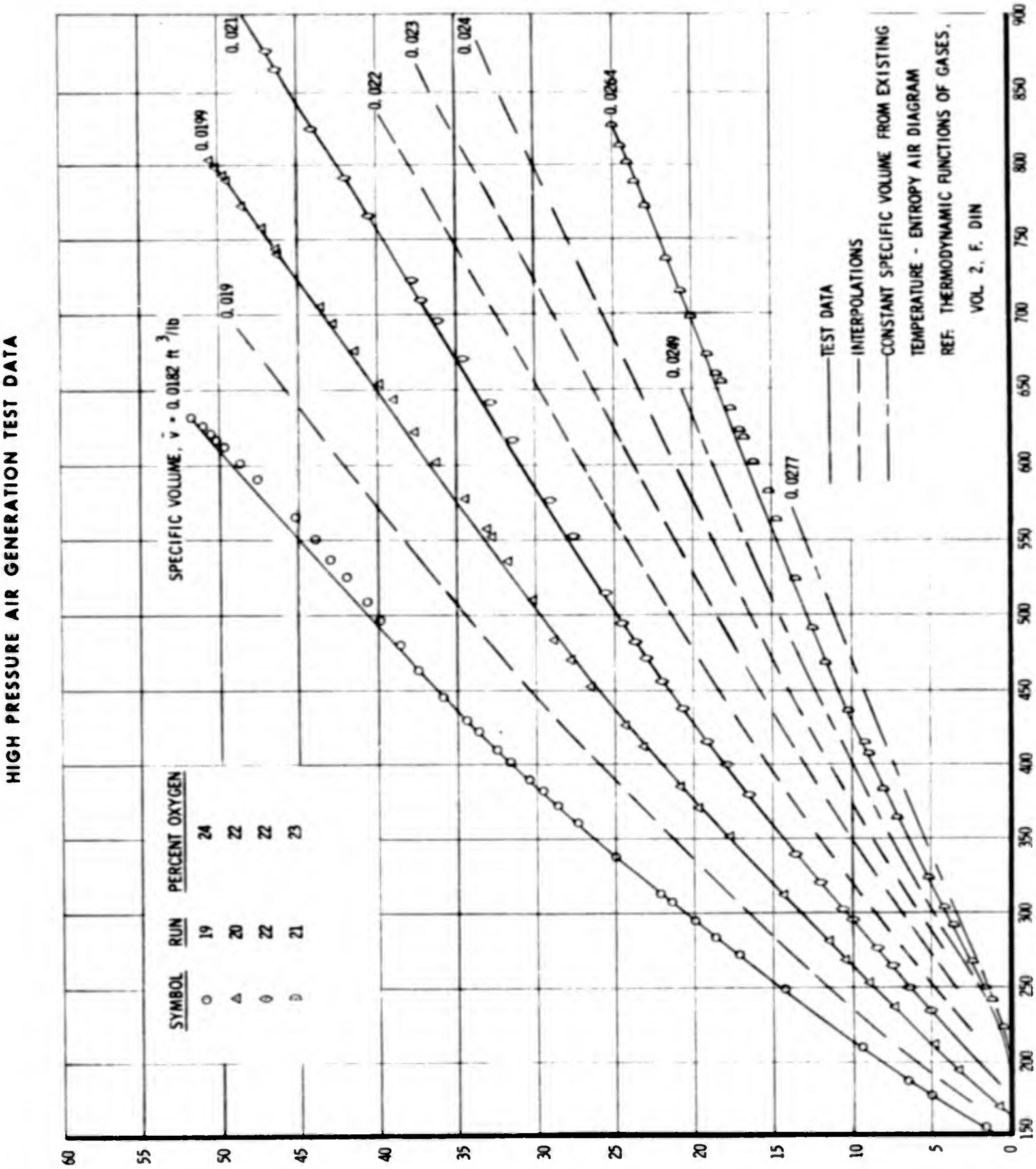

R-17,288

Figure XV-8

volumes during the test program in terms of vessel fluid pressure versus fluid temperature. A close inspection of the curves of Figure XV-8 reveals a departure from the faired line in the temperature region of 500 to 650°R. This variation was determined to result from a temperature gradient existing in the oil bath, in the vertical direction, with a resultant similar temperature gradient (approximately 10-20 degrees) existing in the fluid of the vessel. This temperature gradient of the oil results from free convection heating of the oil since an agitator was not used. However, the accuracy of the curve of each line is assumed to be within 2 percent, because at the end points of each curve, the vessel was allowed to reach equilibrium following draining of the oil. The data in the lower temperature region (150-500°R) is assumed to be within 1 percent because air was used to heat the outside of the vessel, resulting in a more uniform heating of the vessel. Also shown on Figure XV-8 are interpolated data at other specific volumes. The interpolated data were obtained from cross plots of specific volume versus pressure with constant temperature lines. Table XV-II presents the fourth order polynomial equations for a curve fit of the pressure-temperature data of Figure XV-8. The largest percentage deviation from the data curves utilizing the equations was 0.5 percent.

Figure XV-9 presents the air compressibility factor versus temperature, pressure, and specific volume for the test data of Figure XV-8. By graphically differentiating the compressibility factor versus temperature at constant pressure $(\partial Z/\partial T)_p$, sufficient information is available to compute the enthalpy and entropy differences utilizing Equations (2) and (3) (derived in Reference XV-1) and existing Mollier data at 45 cc/mole (Reference XV-2). Appendix A presents the complete listing of calculated differences utilized for extending the temperature-entropy diagrams. Due to the limitation in the amount of data, which affects the accuracy of the graphical differentiation for $(\partial Z/\partial T)_p$, the probable error in the calculated enthalpy and entropy differences is on the order of 2-3 percent.

- -

REFERENCE XV-2 Din, F. "Thermodynamic Functions of Gases" Volume 2

TABLE XV-II

EQUATIONS FOR PRESSURE-TEMPERATURE DATA CURVES

Equation Form: $P = At^4 + Bt^3 + Ct^2 + Dt + E$ (1)

where: P = Pressure in psia

t = Temperature in °R

and: A, B, C, D and E, are constant coefficients

EQUATION CONSTANTS

$\bar{v}$ ft^3/lb	A	B	C	D	E	Applicable Temperature Range °R
0.0182	3.4096×10^{-7}	-4.7278×10^{-4}	1.5285×10^{-1}	1.1691×10^{2}	-1.81901×10^{4}	180-630
0.0199	8.8628×10^{-8}	-1.3163×10^{-4}	2.6699×10^{-2}	1.0097×10^{2}	-1.6570×10^{4}	200-800
0.021	5.1646×10^{-8}	-7.3953×10^{-5}	3.2925×10^{-4}	9.3828×10^{1}	-1.6197×10^{4}	220-880
0.0264	-3.5060×10^{-3}	1.0850×10^{-4}	-1.2436×10^{-1}	9.9649×10^{1}	-1.73345×10^{4}	290-810

The change in enthalpy is calculated as:

$$\Delta H_{2-1} = \left(\frac{Q_1 + Q_2}{2}\right)(P_2 - P_1) \qquad (2)$$

The change in entropy is calculated as:

$$\Delta S_{2-1} = \frac{2(\ln P_2 - \ln P_1)}{W_2 + W_1} \qquad (3)$$

where:

$$Q = -\frac{T^2 R}{P}\left(\frac{\partial Z}{\partial T}\right)_P$$

$$W = \frac{1}{(-TR\,(\partial Z/\partial T)_P - ZR)}$$

T = temperature - °R

R = gas constant - ft/°R

P = pressure - psia

Z = compressibility factor

Figure XV-10 presents the Temperature-Entropy diagram for air extended with the additional data obtained from this test program. The data included from this program are presented as the region bounded by (a) the 33.14 and 45 cc/mole lines, and (b) temperatures of 167°K and 317°K.

Figure XV-11 presents a comparison of data obtained with the vessel completely filled at oxygen content levels of 24 and 32 percent by volume. Also included on Figure XV-11 is the pressure-versus-temperature line for nitrogen obtained from an existing Mollier diagram (Reference XV-3). As seen from Figure XV-11, within the accuracy of the instrumentation, only a slight pressure increase can be noted when comparing the 24 and 32 percent oxygen runs.

- -

REFERENCE XV-3 Din, F. "Thermodynamic Functions of Gases" Volume 3

BLANK PAGE

HIGH PRESSURE AIR GENERATION TEST PROGRAM

COMPRESSIBILITY FACTOR VERSUS TEMPERATURE, PRESSURE, AND SPECIFIC VOLUME

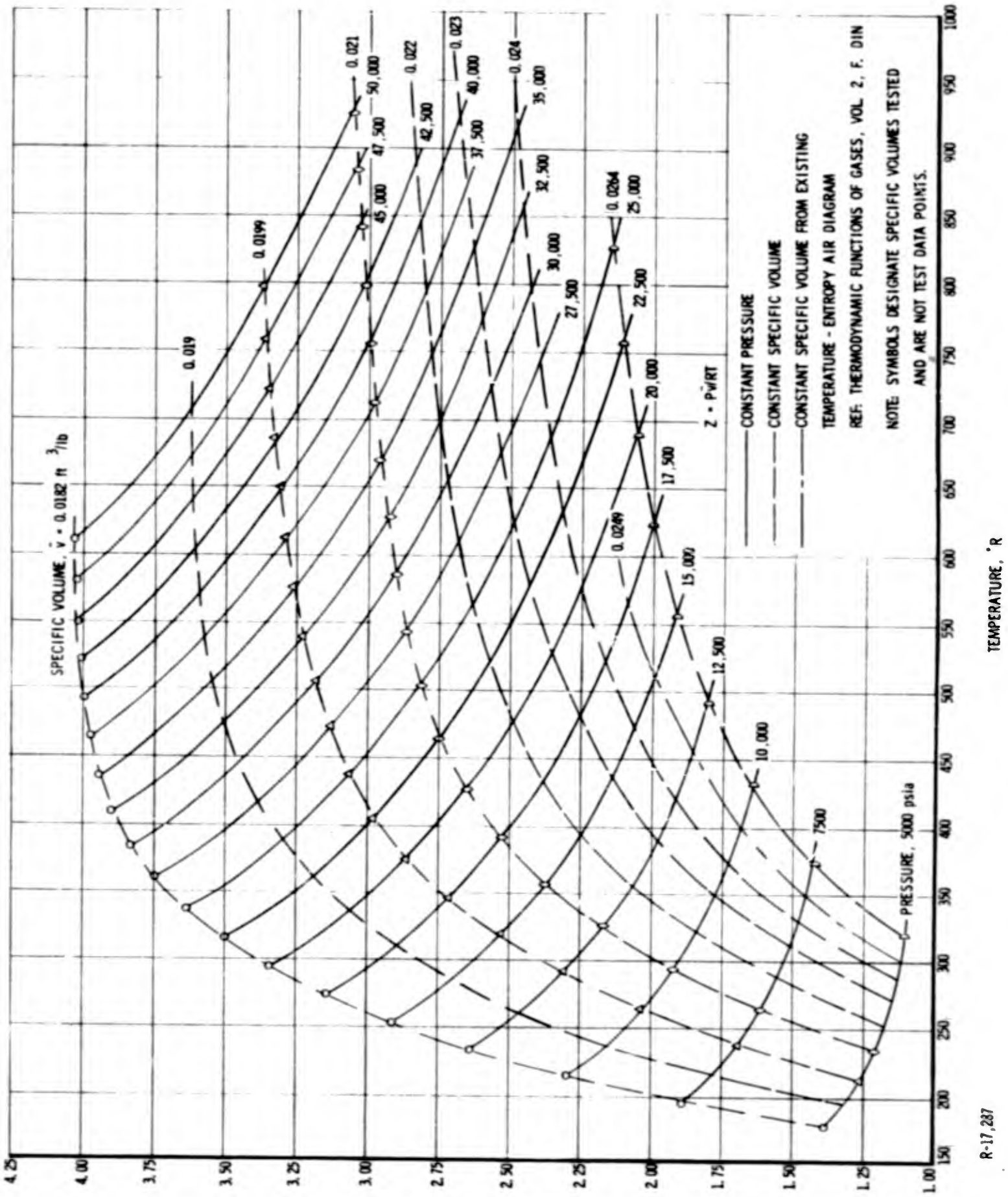

R-17,287

R-17,287

Figure XV-9

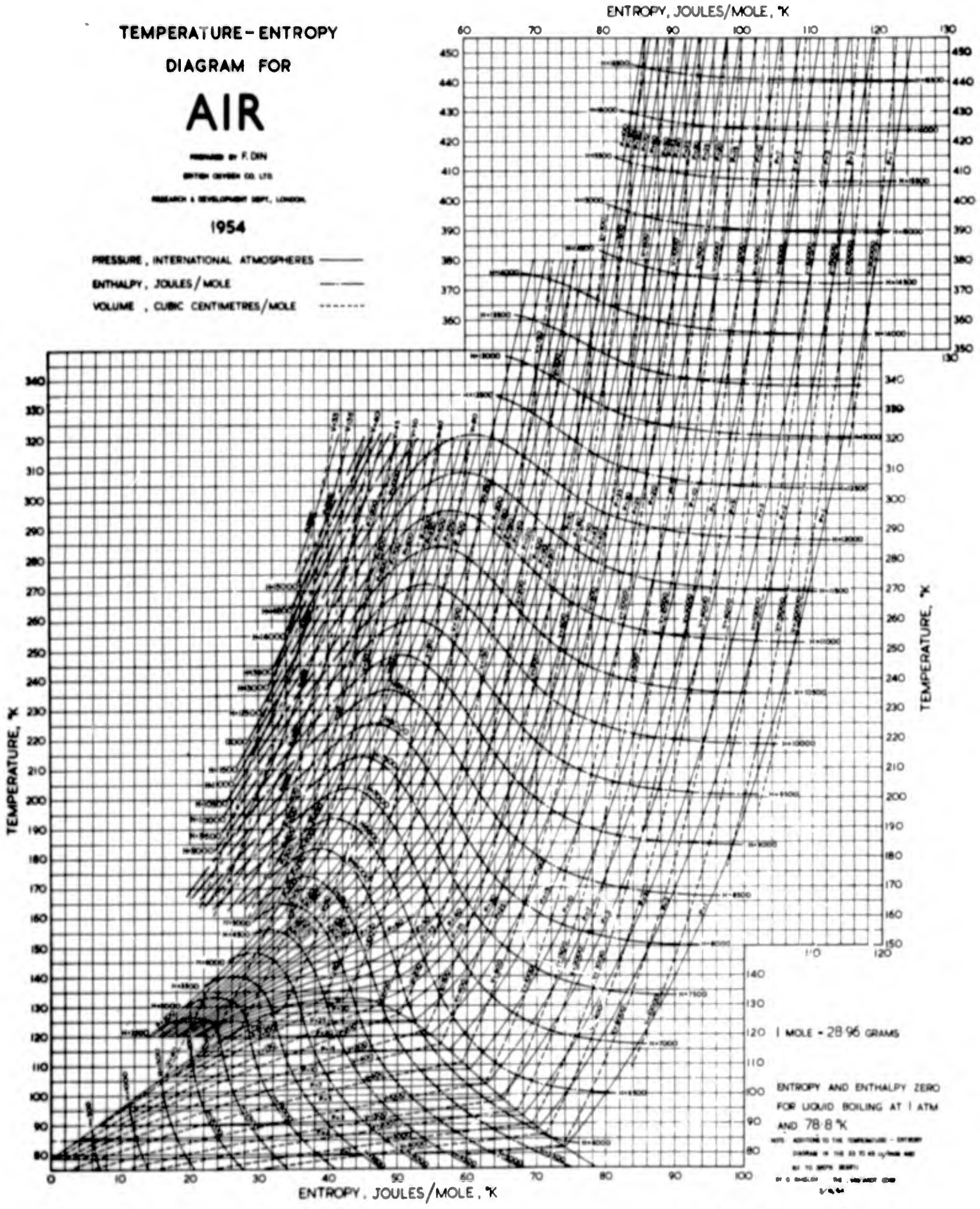
TEMPERATURE-ENTROPY
DIAGRAM FOR
AIR
1954
PRESSURE, INTERNATIONAL ATMOSPHERES
ENTHALPY, JOULES/MOLE
VOLUME, CUBIC CENTIMETRES/MOLE
ENTROPY, JOULES/MOLE, °K
TEMPERATURE, °K
1 MOLE = 28.96 GRAMS
ENTROPY AND ENTHALPY ZERO
FOR LIQUID BOILING AT 1 ATM
AND 78.8°K

FIGURE XV-10

HIGH PRESSURE AIR GENERATION TEST DATA

OXYGEN CONTENT EFFECT ON PRESSURE

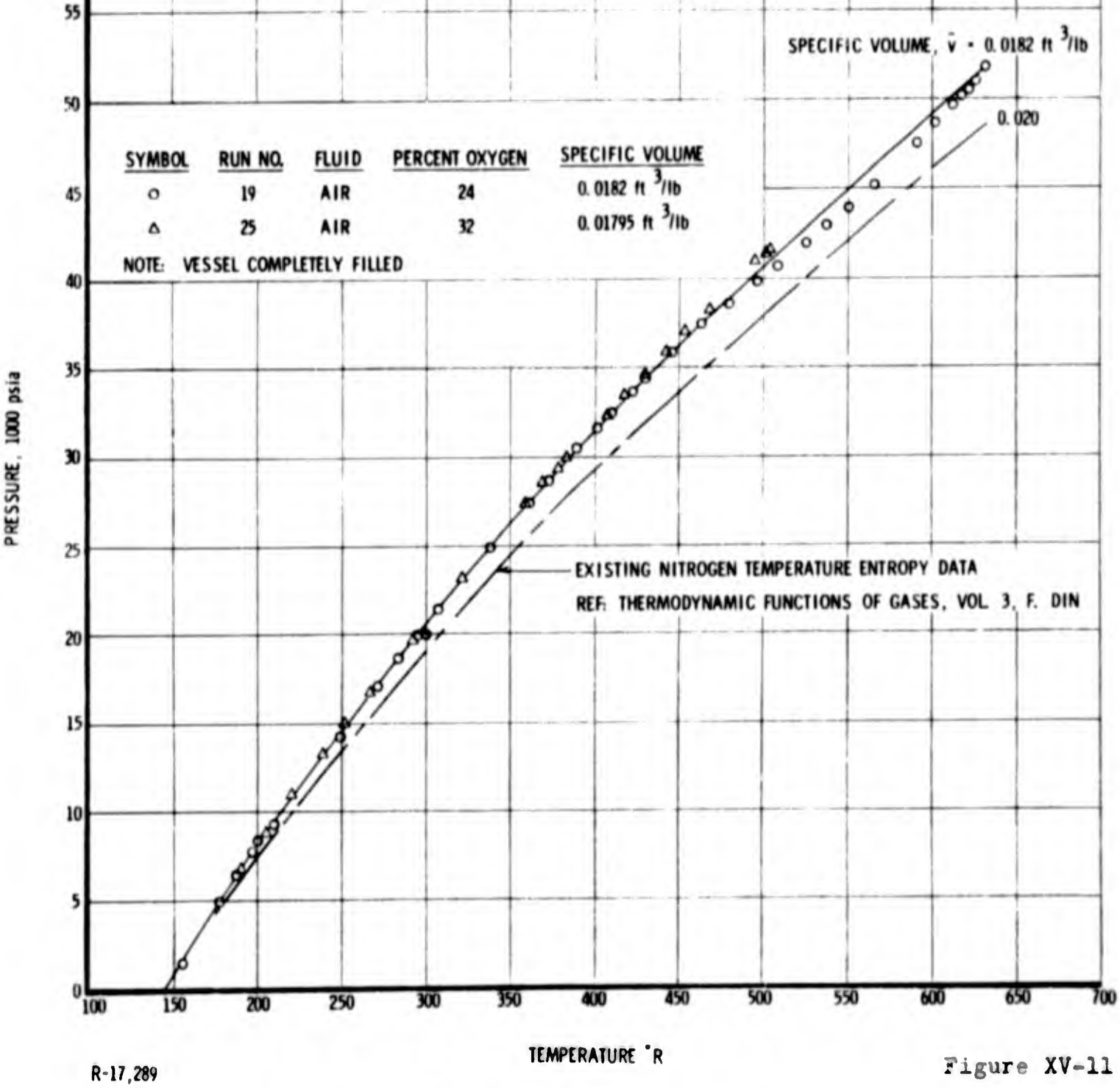

R-17,289

Figure XV-11

This test comparison of oxygen content effects was originally deemed advisable to determine the reason for the various levels of pressure obtained during the CY 1962 test program, where it was assumed that the vessel was completely filled for all runs. However, from the data shown in Figure XV-11, it is apparent that the various levels of pressure obtained during CY 1962 were undoubtedly caused by inconsistent filling of the vessel.

E. Conclusions and Recommendations

1. The test program has successfully demonstrated the practicability of creating extremely high pressures utilizing the principle of heating a cryogenic fluid in a constant volume vessel. A method for obtaining PVT data at pressures in excess of currently available information was utilized to extend existing temperature-entropy data.

2. It is recommended that any subsequent tests to obtain data at extremely high pressures include the following additions:

(a) a method for more uniform heating of the vessel in the temperature region above 500°R should be used,

(b) an investigation should be conducted for other methods of obtaining pressure seals at high pressures during large variations in temperatures since difficulties were experienced with the existing gland nut-cone-seat method, and

(c) additional vessel fluid temperature instrumentation to confirm complete equilibrium of the vessel fluid at all fluid temperatures should be added.

APPENDIX XV-A

ENTHALPY-ENTROPY CALCULATED DIFFERENCES

UTILIZED FOR ADDITIONS TO TEMPERATUE -ENTROPY DIAGRAM

	Specific Volume $\bar{v}$ cc/mole	Temp. T °K	Change in Enthalpy ΔH_{2-1} joules/mole	Enthalpy H joules/mole	Change in Entropy ΔS joules/mole-°K	Entropy S joules/mole-°K	Pressure P tm
Ref. Value	45	167		5200		33.20	340
	40.9		400	5600	-2.60	30.60	510
	38.4		297	5897	-2.31	28.29	680
	36.9		331	6228	-1.88	26.41	850
	35.2		352	6580	-1.60	24.81	1020
	34.1		367	6947	-1.37	23.44	1190
	33.1	167	383	7330	-1.19	22.25	1360
	45	194		6750		37.2	510
	41.6		261	7011	-1.70	35.50	680
	39.3		315	7326	-2.03	33.47	850
	37.6		340	7666	-1.71	31.76	1020
	36.2		355	8021	-1.44	30.32	1190
	34.9		362	8383	-1.27	29.05	1360
	34.0		378	8761	-1.11	27.94	1531
	33.4	194	391	9152	-0.96	26.98	1700
	45	222		8250		40.8	680
	42.1		299	8549	-2.02	38.78	850
	39.9		331	8880	-1.68	37.10	1020
	38.3		350	9230	-1.45	35.65	1190
	37.0		366	9596	-1.28	34.37	1360
	35.8		375	9971	-1.12	33.25	1531
	34.7		377	10348	-1.05	32.20	1700
	34.0		385	10733	-0.92	31.28	1870
	33.4	222	402	11135	-0.79	30.49	2040

APPENDIX XV-A (Continued)

	$\bar{v}$ cc/mole	T °K	ΔH_{2-1} joule/mole	H joules/mole	ΔS joules/mole-°K	S joules/mole-°K	P atm
Ref. Value	45	252		9800		44.0	850
	42.6		326	10126	-1.71	42.29	1020
	40.7		348	10474	-1.46	40.83	1190
	39.1		368	10842	-1.24	39.59	1360
	37.8		382	11224	-1.11	38.48	1531
	36.6		383	11607	-1.01	37.47	1700
	35.6		38[illegible]	11992	-0.93	36.54	1870
	34.[illegible]		390	12382	-0.85	35.69	2040
	33.97		396	12778	-0.76	34.93	2210
	33.4	252	413	13191	-0.64	34.29	2380
	47.75	281	-263	10987	+1.36	47.96	885
	45			11250		46.6	1020
	42.9		+348	11598	-1.45	45.15	1190
	41.1		372	11970	-1.25	43.90	1360
	39.6		378	12348	-1.10	42.80	1531
	38.2		390	12738	-1.00	41.80	1700
	37.2		395	13133	-0.98	40.92	1870
	36.2		395	13528	-0.89	40.09	2040
	35.3		394	13922	-0.77	39.32	2210
	34.5		399	14321	-0.72	38.60	2380
	33.9		404	14725	-0.64	37.96	2550
	33.4	281	419	15144	-0.56	37.40	2720

APPENDIX XV-A (Continued)

	$\bar{v}$ cc/mole	T °K	ΔH_{2-1} joule/mole	H joules/mole	ΔS joules/mole-°K	S joules/mole-°K	P atm
Ref. Value	47.75	316	-315	12685	+1.26	50.76	1050
	45			13000		49.50	1210
	43.2		+323	13323	-1.11	48.39	1360
	41.4		394	13717	-1.08	47.31	1531
	39.98		396	14113	-0.89	46.34	1700
	38.8		403	14516	-0.86	45.48	1870
	37.6		407	14923	-0.80	44.68	2040
	36.7		402	15325	-0.74	43.94	2210
	35.9		400	15725	-0.71	43.23	2380
	35.2		400	16125	-0.68	42.55	2550
	34.4		397	16522	-0.62	41.93	2720
	33.9		403	16925	-0.59	41.34	2890
	33.3	316	419	17344	-0.49	40.85	3060